BRNO UNIVERSITY OF TECHNOLOGY
VYSOKÉ UČENÍ TECHNICKÉ V BRNĚ

FACULTY OF CHEMISTRY
FAKULTA CHEMICKÁ

INSTITUTE OF PHYSICAL AND APPLIED CHEMISTRY
ÚSTAV FYZIKÁLNÍ A SPOTŘEBNÍ CHEMIE

PRINTED BIOSENSOR BASED ON ORGANIC ELECTROCHEMICAL TRANSISTOR
PRINTED BIOSENSOR BASED ON ORGANIC ELECTROCHEMICAL TRANSISTOR

DOCTORAL THESIS
DIZERTAČNÍ PRÁCE

AUTHOR — Ing. Lukáš Omasta
AUTOR PRÁCE

SUPERVISOR — doc. Ing. Ota Salyk, CSc.
ŠKOLITEL

BRNO 2019

ABSTRACT

Organic electronic devices arise as a suitable solution for bioelectronics sensor development, due to the good biocompatibility of organic semiconductors. So-called biosensors can convert electrochemical processes into an electronic signal. A matrix of such biosensors can simultaneously scan a number of biological samples or tissues of the living systems. The active part of the device is an Organic Electrochemical Transistor (OECT). In this work, the theoretical background on such device and its characterization, application in cell-based biosensors, methods of fabrication together with the current state of the art in the field of organic electronics are discussed.

The experimental part contains specific manufacturing procedures of OECT devices development employed. The main emphasis is given on the ability of produced devices to detect response and monitor the stimulation of electrogenic cells. To this end, microplate patterns with a multielectrode array of OECTs based on the semiconductive polymer PEDOT:PSS was developed and fabricated using conventional printing methods (inkjet printing and screen printing). Standard lithographic procedures were also employed. The latest devices with the highest achieved signal amplification of $g = 2.5$ mS and the time constant of $t = 0.15$ s were produced. These are comparable or even better than some state of the art fully lithographically prepared ones.

ABSTRAKT

Organické elektronické zariadenia sú vyvíjané ako vhodné riešenia senzorov pre bioelektroniku, a to najmä kvôli dobrej biokompatibilite organických polovodičov v nich použitých. Takzvané biosenzory dokážu premeniť elektrochemické procesy na elektronický signál. Matrica takýchto biosenzorov môže simultánne skenovať množstvo biologických vzoriek, alebo rôznych tkanív v živých systémoch. Aktívnou súčasťou zariadenia je organický elektrochemický tranzistor (OECT). V tejto práci je diskutovaný teoretický rámec fungovania takéhoto zariadenia, jeho elektrická charakterizácia, aplikácia v biosenzoroch na báze buniek, spôsoby výroby a aktuálnym stavom techniky v oblasti organickej elektroniky.

Experimentálna časť obsahuje konkrétne výrobné postupy vývoja OECT zariadení, ktoré boli použité v našom laboratóriu. Hlavný dôraz sa kladie na schopnosť vyrobených zariadení detekovať reakciu a monitorovať stimuláciu elektrogenných buniek. Za týmto účelom boli vyvinuté matice mikroelektródových OECT zariadení založených na polovodivom polyméri PEDOT:PSS. Tieto boli vyrobené s využitím bežnými tlačiarenských techník (atramentová tlač a sieťotlač) spolu so štandardnými litografickými postupmi. Najnovšie nami vyvinuté zariadenia dosahujú najväčšieho zosílením signálu, $g = 2{,}5$ mS a časovú konštantu $t = 0{,}15$ s. Tieto zariadenia sú porovnateľné, často dokonca lepšie ako niektoré iné najmodernejšie a plne litograficky pripravené senzory.

KEYWORDS

Organic electrochemical transistor, inkjet printing, screen printing, printed electronics, biosensor, PEDOT:PSS

KĽÚČOVÉ SLOVÁ

Organický elektrochemický tranzistor, atramentová tlač, sieťotlač, tlačená elektronika, biosenzor, PEDOT:PSS

CONTENT

AIM AND MOTIVATION

The aim of this dissertation thesis is a comprehensive overview of organic electrochemical transistors and their use as a bioelectronic sensor. Human cell cultures provide a potentially powerful means for pharmacological and toxicological research. Electrogenic cell cultures are advantageously studied by the means of OECTs. They are promising transducers for bio-interfacing. This is due to their biocompatibility, high transconductance, and the possibility of manufacturing in all manner of structures and designs.

Most OECTs reported to date, however, are produced using lithographic techniques with the need for clean room facilities. These standard manufacturing processes are costly, lengthy and the production rate is rather slow. We aimed to alleviate the aforementioned production drawbacks by introducing standard printing techniques, such as inkjet printing and screen printing. Such an envisioned platform is produced cheaply and in large quantities, without the need for cleanroom facilities. It is accessible and easy to implement during routine cell culture measurements.

1 INTRODUCTION

The field of organic electronics has grown significantly in the past twenty years. It has been so mainly because of the many desirable properties of organic semiconductors. Among the most notable are the low cost, ease of processing and their ability to be tuned through synthetic chemistry [1]. Organic electronics can link the fields of electronics and biology, as organics have the ability to conduct both electronic and ionic charges with significant mobility at room temperature. This important property is leveraged in a variety of devices that utilize mixed electronic/ionic conduction [2]. For example, the dimensional changes caused by ion injection can be used to build mechanical actuators, also known as artificial muscles. Ion redistribution within a layer conveys electronic charge injection from metal electrodes. This effect can be utilized to achieve efficient electroluminescence in light-emitting electrochemical cells [3]. In electrochromic displays, ions injected from an electrolyte change the colour of a polymer film [4]. Furthermore, ion diffusion across an interface is used to control the energetics of the heterojunction, thus forming diodes [5]. Mixed electronic/ionic conductivity is of particular importance for devices that interface electronics with biology, a subject that is currently attracting a great deal of attention [6]. The intention of organic bioelectronics is to address the current and future diagnostic and therapeutic needs of the biomedical community [7], [8]. These needs include for instance improving compatibility with the biological environment. Also important is the detection of low concentrations of biological analytes, and pathogens, as well as detection of low amplitude brain activity. Electrical methods for biological sensing are considered favourable, in particular, due to the fact that they are label-free. They also do not require expensive and time-consuming techniques which involve fluorophores or chromophores.

Present diagnostic approaches using electrical sensors involve large-scale integrated systems, passive metal electrodes, and electrochemical biosensors. Operating principle of these systems is based on changes in the impedance, local potential or redox reactions. However, for electrochemical sensors, the biological signals are often difficult to record and demand further amplification to become detectable. That is why a push toward more active, sensitive, and biocompatible devices is necessary [9], [10].

As lab-on-chip arrays for biomedical applications become more and more sophisticated by increasing the number of fluidic, electronic, and mechanical components, space and design restrictions become more important [11]. Organic thin film transistors (OTFT) provide unique opportunities when integrated into these systems as transducers that can be easily patterned, individually functionalized, and directly interfaced with biomolecules and living cells. Organic electrochemical transistors (OECTs) as a subset of OTFT have distinguished themselves in recent years due to their simple fabrication and low voltage operation [12]. The ability to operate in aqueous environments and the integration with microfluidics make OECTs excellent candidates for a variety of applications, especially in the area of sensing and biosensing.

2 THEORETICAL PART

The following chapters deal in detail with organic electrochemical transistors, its physics, circuit model and geometry. The role of PEDOT:PSS as the most commonly used material is discussed together with the current state of the art and potential use of OECTs in bioelectronics.

2.1 ORGANIC ELECTROCHEMICAL TRANSISTORS

White et al. firstly demonstrated OECTs, in which the conductivity of a polypyrrole film was modulated by the application of a gate voltage through an electrolyte [13]. Since the invention of OECTs as a variant of the OTFT, it became a promising device for biocompatible sensors in biology and medicine. The growing area of bioelectronics, which links the fields of electronics and biology, holds immense potential for the development of innovative biomedical devices for therapeutics and diagnostics. OECTs can be used as logic elements, as well as incorporated into microfluidics, or coupled to bilayer membranes with ion channels. They can also be used for sensing of water vapour, deoxyribonucleic acid, glucose and lots of other analytes.

Biosensors arose as a promising solution for the investigation of processes in cells and tissue cultures in vitro as well as for diagnostic and therapy in vivo. OECTs are designed to convert the electrochemical processes at cell membranes to electronic signals. Application of organic electronics brings the new approach for sensing in biology and medicine. The central part of the device is a transistor, nowadays mostly based on PEDOT:PSS (poly(3,4-ethylenedioxythiophene) polystyrene sulfonate) conductive polymer.

Electrochemical polymerization of conductive polymer PEDOT was firstly reported back in 1992 by Heywang et al. [14]. The first PEDOT:PSS co-polymer was prepared by the potentiostatic electrochemical polymerization in 1995 by Yamato et al. [15]. PEDOT:PSS has outstanding biocompatibility and potentially high device amplification. Solid or gel electrolyte based devices have been prepared and show similar behaviour to solution based ones.

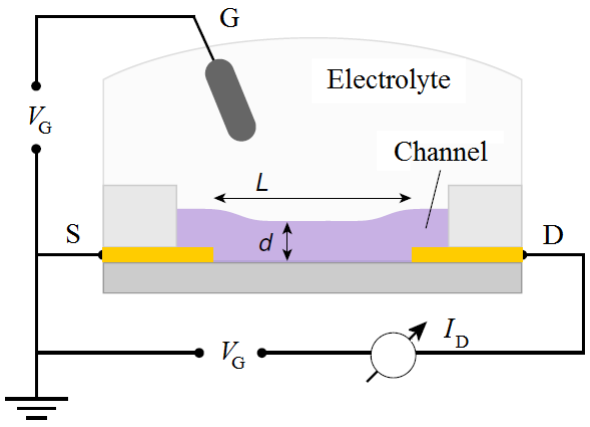

Figure 1 The typical structure of an organic electrochemical transistor (OECT), showing the source (S), drain (D), electrolyte and gate (G) [17]

The semiconducting PEDOT is p‑type doped (oxidized form), which leads to mobile holes that can jump from one chain to another, resulting in a hole current. These holes are compensated by sulfonate anions of PSS, which can be considered as ionized acceptors [16]. In the absence of a gate voltage, a hole current flows in the channel (that is, the ON state), this means that OECTs based on PEDOT:PSS operate in depletion mode. By applying a positive gate bias, cations from

the electrolyte are injected into the channel, and the anions are compensated. This is comparable to compensation doping and as a result, the number of holes in the channel decreases. The channel is de-doped as the holes that are extracted at the drain are not replenished at the source. This manifests as a drop in the drain current, and the device reaches the OFF state (Figure 2) [17].

The OECT crucial feature is that doping changes occur over the entire volume of the channel which is in contrast to the field-effect transistors (FETs) where de-doping changes occur only in the interfacial region. OECTs are efficient switches and powerful amplifiers due to the large modulations in the drain current, which can be achieved by applying low gate voltages [18], [19], [20]. The use of electrolytes results in the tremendous flexibility in device architecture and integration with a range of different substrates, utilizing a variety of form factors and a wide range of fabrication processes. The fundamental adjustability of organic molecules allows further optimization of ion and electron transport and simplifies bio-functionalization. Thanks to these characteristics, OECTs are investigated and tested in various applications, including neural interfaces [21], [22], chemical and biological sensors [23], [24], printed circuits [25], [26] and neuromorphic devices [27], [28].

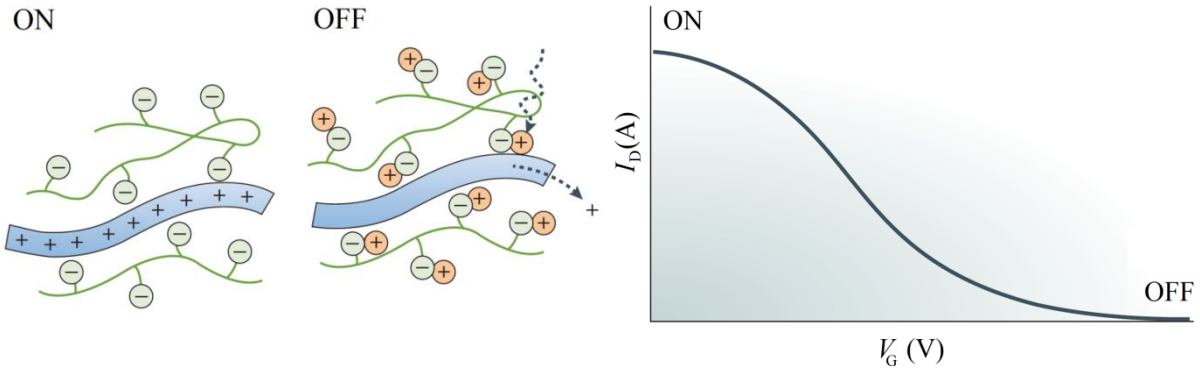

Figure 2 Transfer curve showing the depletion-mode operation of an OECT with a conducting polymer channel [20]

2.1.1 The device physics of OECTs

OECTs transduce small voltage signals applied to the gate into large changes in the drain current. This transduction process is described by a transfer curve, which shows the dependence of the drain current on the gate voltage (Figure 3). The steeper the transfer curve, the more significant the change in drain current for a given gate voltage signal.

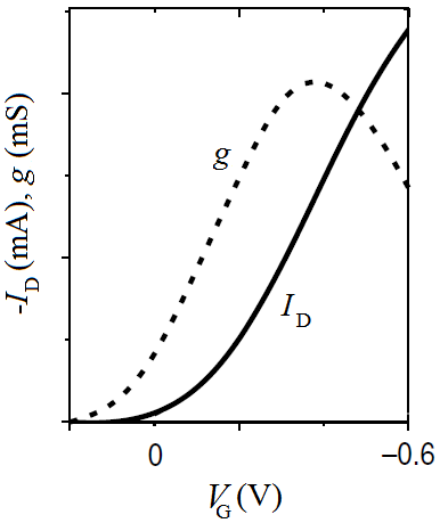

Figure 3 The depiction of the typical OECT transfer curve I_D together with transconductance g [20]

The effectiveness of transduction is determined by the first derivative of the transfer curve and is called transconductance:

$$g = \partial I_{\mathrm{D}} / \partial V_{\mathrm{G}} \tag{1}$$

The most critical parameter for electrochemical transistors to consider and evaluate is transconductance. OECTs have very high transconductance values, on the order of millisiemens (mS) for micrometer-scale devices [18]. This is due to the volumetric nature of the response of these devices. The basic physical model of OECT operation was described by Bernards [17]. This model captures and describes both steady and transient state of the OECTs. It concludes that ions from the electrolyte enter the channel and change the electronic conductivity throughout its volume. The OECT can be divided into two circuits: electronic, which describes the flow of electronic charge in the source–channel–drain structure according to Ohms law. The second one: the ionic circuit, which describes the flow of ions in the gate–electrolyte–channel structure (Figure 4). The electronic circuit can be understood as a resistor, in which electronic charge drifts under the influence of the local potential as in the case of MOSFETs (Metal Oxide Semiconductor Field Effect Transistors). The ionic circuit is made of a resistor in series with a capacitor. Resistive part explains the flow of the ions in the electrolyte, and the capacitive part describes the storage of ions in the channel. Using this model, we assume that ions which are injected into the channel do not transfer charge through the OECT film. Hence this model describes utterly capacitive behaviour. Ions electrostatically compensate the opposite charges presented in the conductive channel replacing holes localized on the PEDOT backbone.

We assume that no electrochemical reaction takes place between the electrolyte and the channel. At the steady state, the capacitor is charged, and the gate current approaches zero due to the lack of holes as the charge carriers. Bernard's model gives us a good fit for the output characteristics of OECTs and allows quantitative predictions of the transconductance g At saturation and for depletion-mode devices, it gives [17]:

$$g = (W/L) \cdot d \cdot \mu \cdot C^{*} \cdot (V_{\mathrm{Th}} - V_{\mathrm{G}}) \tag{2}$$

Where W, L, and d is the channel width, length, and thickness, respectively; μ is the charge-carrier mobility; C^* is the capacitance per unit volume of the channel, and V_{Th} is the threshold voltage. The voltage terms are inverted in the case of accumulation-mode OECTs. This equation is comparable with the one for FETs, the difference here is that the product $d \cdot C^*$ substitutes the capacitance per unit area of the MOS (Metal Oxide Semiconductor) capacitor, C'. This modification characterizes the difference between these two architectures. The physical thickness of the channel does not affect the conductivity of the FET devices.

On the other hand in an OECT, the channel thickness is a parameter that can modify their output. Volumetric gating makes OECTs to perform better regarding amplification in comparison with other transistor types and architectures [18]. The high transconductance of OECTs is unfortunately compensated by their rather large time constants.

From Bernard's model, we can anticipate that the response time will be limited by either the ionic or the electronic circuit. In most cases, the ionic circuit controls the response time, which is determined by the product of the resistance of the electrolyte and the capacitance of the channel. The capacitance of the channel is proportionate to the thickness of the channel. This results in the slower OECT operation as the thickness d of the channel is getting bigger [17]. Therefore the thickness of the channel can be used as a variable when deciding between gain and bandwidth [22]. Typical response times of micro-fabricated OECTs with liquid electrolytes are in the range of milliseconds. The application possibilities of OECTs are therefore limited, especially concerning the frequency range with the maximum of tens of kilohertz (kHz). This is sufficient for most biosensor applications, which is quasi-static, and for recording electrophysiological signals [17]. In case of solid or gel electrolytes, the response time is even larger, but many applications, particularly in the field of printed electronics, do not require fast response times [29].

Bernard's model can be improved by taking into consideration, for example, variable conductivity along the OECT channel, which is nonlinearly dependent on the charge density. This was observed using spatially resolved voltage measurements along the OECT channel [12]. Non-ideal contacts in OECTs introduce additional complications [30]. A more precise characterization of the transfer curve can be done by considering the influence of disorder on hole transport in the channel [31]. Another consideration is that OECTs accounts for the limit at which ions freely enter the volume of the channel. This has been demonstrated in various materials, in which capacitance is proportional to the film thickness [19], [32].

On the other hand, electrolyte-gated FETs account for the other extreme in which ions accumulate at the surface of the channel. Several materials exhibit a response between the two extremes [33]. This suggests the presence of a barrier for ion injection. The physics of electron and hole injection and transport in organic semiconductors has been widely studied in previous decades. Nevertheless, not that much is known about the processes of ion injection and transport in organic semiconductors.

As a result of the electrolyte gating in the OECTs, the fraction of the applied gate voltage that drops across the channel is controlled by the nature and geometry of the gate electrode [34]. Two capacitors are formed in the ionic circuit if a polarizable electrode is used as the gate (Pt or Au). One capacitor represents the electrical double layer formed at the gate–electrolyte interface, and the other capacitor corresponds to the volumetric capacitance of the channel.

The capacitors are connected in series. Therefore the applied gate voltage drops across the smaller one of these two (Figure 4). The capacitance of the gate electrode must be more than ten times larger than the capacitance of the channel to achieve efficient gating. If it is not the case, then a significant fraction of the applied gate voltage will drop at the gate–electrolyte interface.

Large gate capacitance can be achieved for example by using thick PEDOT:PSS electrode as the gate electrode.

Another approach is to use a non-polarizable gate electrode (Ag/AgCl). In this case, the voltage drop at the gate–electrolyte interface is insignificant [35]. The type of the electrolyte: liquid, gel or solid and the ion concentration have an impact on the response time of the transistor as well. This is because the electrolyte conductivity determines the resistance of the ionic circuit [36].

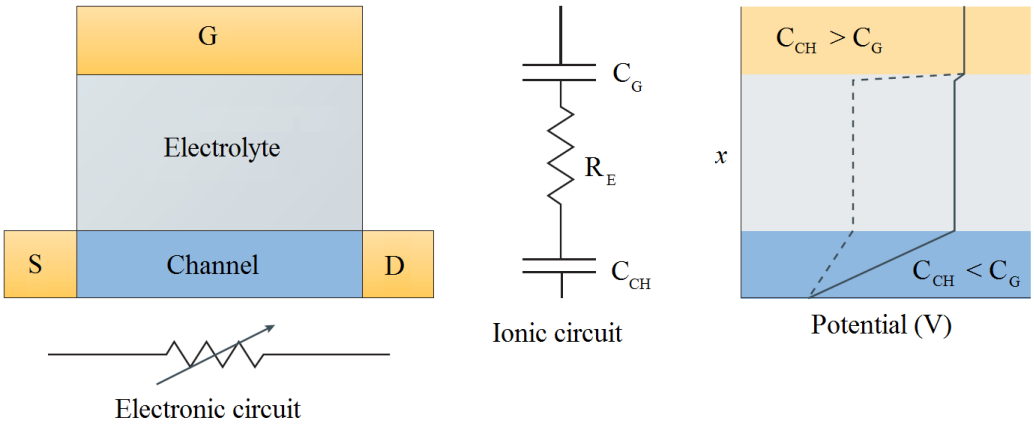

Figure 4 Ionic and electronic circuits used to model OECTs [20]

The electronic circuit, shown below the device design on the left, is modeled as a resistor with a resistance dependent on the applied voltage at the gate electrode. The ionic circuit, depicted in the middle, is composed of the capacitors corresponding to the channel (denoted C_{CH}) and gate (denoted C_G) and a resistor corresponding to the electrolyte (denoted R_E), respectively. The distribution of potential in the ionic circuit is illustrated on the right. The solid line represents the case of effective gating. At this point, ions are driven inside of the channel because most of the applied gate voltage drops at the boundary between the electrolyte and the channel. The dashed lines, on the other hand, represent the case of ineffective gating, where most of the applied gate voltage drops at the gate–electrolyte interface.

2.2 OECT GEOMETRY

The volumetric character of the capacitance of the OECTs has a particular effect on a relationship between the transconductance and the device geometry (Figure 5). This is well illustrated by equation (2). From the previous research done by Rivnay et al. it can be deduced that the transconductance at saturation is proportional to the term Wd/L [22][22]. The response time τ is also given by the volumetric response of capacitance and therefore by the device geometry.

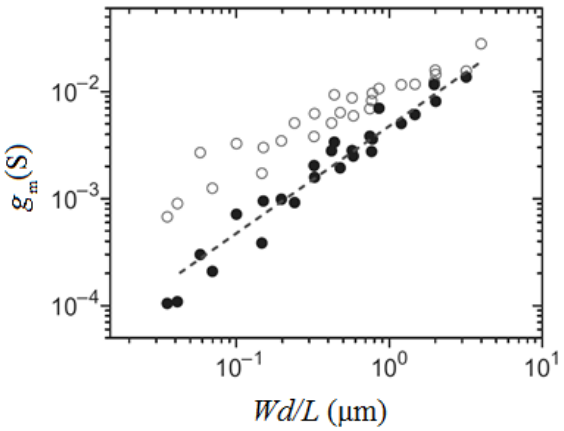

Figure 5 Dependence of the OECT transconductance on the device geometry. Open symbols correspond to peak transconductance, and solid symbols are the transconductance at saturation equation (2) [22]

The most prominent feature of OECTs which distinguishes them from classical FETs is the increase/decrease of transconductance with a higher/lower thickness of the channel respectively. This relationship was proven in devices with layer thickness up to 1 mm. Deviations from this relationship may be assumed for layers with a greater thickness with respect to second order effects (for example, incomplete film hydration).

This makes OECTs excellent candidates for applications in which channel area is fixed by geometrical constraints, such as recording arrays, where devices must be tightly packed, and lab-on-a-chip systems, where space is very tight [22].

3 STATE OF THE ART

Conventional and also unconventional methods and approaches in the field of printed electronics have been explored to manufacture OECT devices and circuits on various substrates, most notably plastic foils, and paper. These techniques include screen printing [40] and inkjet printing [41].

All screen printed OECT logic circuits, and shift registers have been manufactured on flexible substrate poly(ethylene terephthalate) (PET) [26]. An OECT device prepared on an ultrathin parylene substrate has been published and intended as a sensor in bioelectronics [21]. OECTs prepared on textiles also have their potential, primarily as an application in the field of wearable electronics. PEDOT based OECT was utilized in the preparation of gas sensors on Gore-Tex which served as a "breathable" substrate [42]. Other common types of fabrics, such as woven cotton and Lycra have been used as substrates for screen printed wearable sensors for sensing of the external biological fluid (sweat, saliva, urine) [43].

3.1 OECT APPLICATIONS IN BIOELECTRONICS

OECTs represent an essential part of research in the field of bioelectronics, healthcare, and biomedicine [10], [20]. OECTs can be interfaced with various cells, tissues and living organs in the study of their electrical properties (electrophysiology) to measure cell activity. Due to the local signal amplification, the activities of deep brain tissue or epileptic seizures can be observed using microfabricated OECTs, which can be placed directly on the brain of a living rat. In other published works, OECTs have been demonstrated in mediating the contact between the conducting channel and cerebrospinal fluid. This allows using OECTs to inject current and stimulate neurons locally [44]. Another example are OECTs coupled with OFETs which can record myograms with high temporal resolution in rats [45]. Epidermally applied OECTs can for instance record an electrocardiogram when placed on the human skin [46].

An integral part of these measurements is the cultivation of the cell monolayer which covers the channel. This, in turn, results in the formation of a barrier for ion motion and insertion into the channel altering the characteristics of the OECTs [50]. A similar basis can be employed to evaluate ion channels in lipid bilayers assembled on PEDOT:PSS channels [51]. Another advantage of PEDOT:PSS based OECTs is the possibility of simultaneous analysis of optical and electronic signals, due to the fact that PEDO:PSS is optically transparent in the visible part of the electromagnetic spectra [52]. Worth mentioning is also the fact that OECT can operate in various intricate environments, for example, milk where they can detect the pathogens by measuring transepithelial ion flow [53]. OECTs can be coupled with 3D cell cultures to monitor their integrity and the effect of several toxic compounds on the cell structure. It is also possible to control the location of epithelial cells attachment on the channel by the variation in an applied drain and gate voltage [54]. This offers the opportunity not only to monitor but also control cell behaviour as was shown using porous sponge-like PEDOT:PSS scaffold able to sustain and control cell culture attachment [55].

3.2 OECT IN CELL SENSING APPLICATIONS

The integration of OECTs with living cells has concentrated on the sensitivity to the changes in biological ion flux. This indicator is used for monitoring the integrity of mammalian cells. The flow of ions is regulated in tissues and dysregulation is often a sign of disease or dysfunction. OECTs have been used for sensing barrier tissue integrity and changes in paracellular ion flux.

Another way to measure the integrity of cells is to seed the cells directly on a device. This can be done using a top-gate device structure, or side-gate structure. The top-gate structure was used by Lin et al. [56], and the device was able to detect cell attachment and detachment by shifting the V_g values. The constant operation of the OECT in cell culture together with the ability to facilitate cell growth was validated by Yao et al. [48].

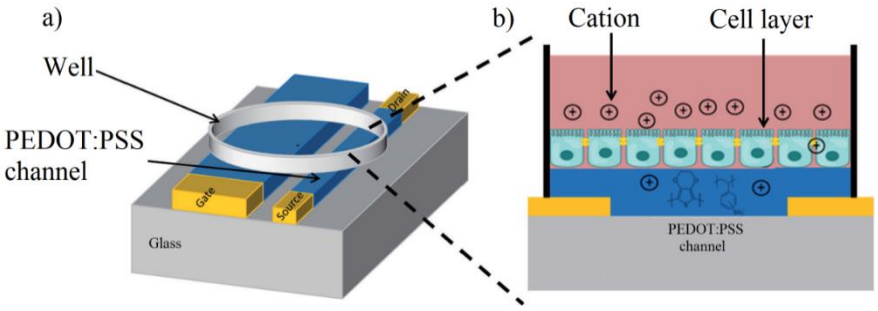

Figure 6 Schematic of the device which consists of a PEDOT:PSS channel and gate patterned onto a glass slide. Cells and media are contained inside a 3D-printed PDMS (polydimethylsiloxane) well [48]

Electrical stimulation and recording of neural activity and nerve tissue have provided invaluable information, mainly in the area of pathological and physiological functions of the body and brain.

The primary technique to record cardiac activity, electrocardiography (ECG), uses electrodes in contact with the skin which provides information about the normal function or abnormalities of the heart. Campana [46] fabricated OECTs on flexible, resorbable PLGA poly(lactic-co-glycolic) acid substrates for ECG recordings.

For the brain, there are three principal electrophysiology recording methods, electroencephalography (EEG), electrocorticography (ECoG), and stereoelectroencephalography (SEEG).

Khodagholy et al. [21] demonstrated and published OECTs for ECoG recordings that can be directly implanted. A conformal device, consisting of integrated electrodes and OECTs array, was placed on the surface of the brain of an epileptic rat. This demonstrated that OECTs could detect low-level activity that was poorly detectable with surface electrodes. This type of devices can be potentially implemented in curing epilepsy, where the identification of zones generating high-frequency oscillations or micro-seizures is critical for diagnosis. In a recent publication the use of an OECT to monitor cardiac rhythm, eye movement, and brain activity in a human volunteer have also been accomplished [47].

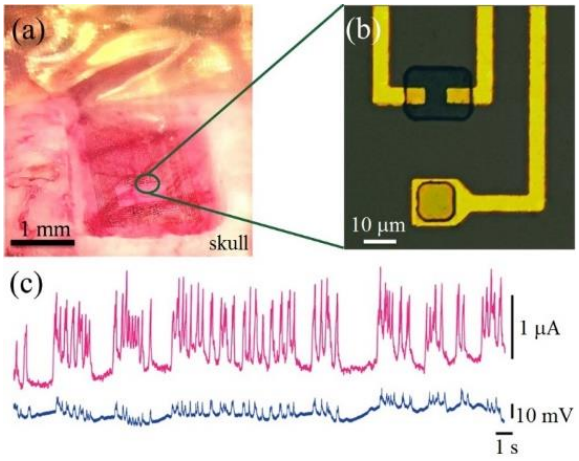

Figure 7 Optical micrograph of an array carrying OECTs and electrodes, placed over the somatosensory cortex (a) and detail of the transistor and electrode structures (b). Recordings from an OECT (top) and an electrode (bottom) show the superior recording ability of the former (c) [10]

Another example is the use of a 16-channel OECT array to map the field potential conduction of a primary rat cardiomyocyte monolayer [49]. Acquisition of the essential parameters in studying cardiac electrophysiology such as the heartbeat frequency, direction, and velocity of the propagation of FPs, the FP duration, and FP rise time has been recorded. These parameters are crucial to quantitatively describe the FP characteristics as was discussed previously.

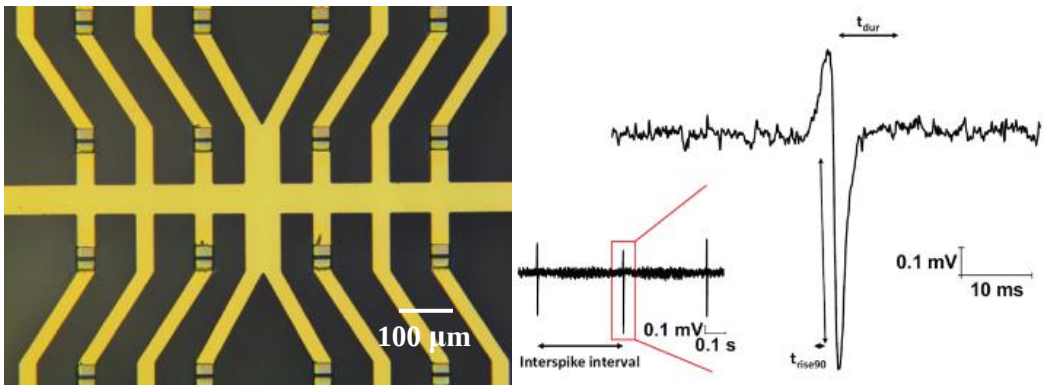

Figure 8(Left) lithographically fabricated multi-OECT device. (Right) The profile of a single field potential of measured cardiomyocytes [49]

4 METHODS

In this chapter, a brief description of the manufacturing methods used in this thesis to produce OECT devices is presented. Specifically described herein are photolithography techniques used to prepare the negative photoresist layer SU-8 and the two printing methods (inkjet printing and screen printing) used to produce conductive, semiconducting and insulating layers.

4.1 INKJET PRINTING OF ORGANIC ELECTRONIC

The basic idea of inkjet printing is to print graphical images by firing tiny droplets of ink onto a substrate. Inkjet printing can be used as a combined deposition and patterning technique in the area of organic electronics. It is a noncontact, maskless, relatively fast and cheap technique. Inkjet printing has found its best uses in combination with other patterning techniques.

Applications of the inkjet technique include studies focused on the printing of hole interconnections in polymer thin film transistor circuits [58], the modification of the sheet resistivity of PEDOT:PSS electrodes [59], the printing of polymer field effect transistors [60], the printing of capacitors and the printing of the pixels in polymer displays. Inkjet printing of conjugated polymers has been done primarily by using advanced inkjet printing devices. On the other hand, several research groups are using simple desktop printers for device fabrication as well.

4.2 SCREEN PRINTING OF ORGANIC ELECTRONICS

The first developments of screen printing date back to the beginning of the 20th century. It is a versatile printing technique that allows for full 2-dimensional patterning of the printed layer. Screen printing is used to manufacture several types of large graphics, posters and also writing on a printed circuit board. It is a simple technique compatible with various materials and surfaces of substrates.

The screen printing device is shown in (Figure 9), and it involves a screen of woven material (synthetic fiber, steel mesh) glued to a frame. The printing pattern is realized by filling the screen printing mesh with a coating emulsion. The area of the printed pattern is kept open, without the emulsion. A squeegee is used to force printing paste through the screen and thus to reproduce the printing pattern onto the substrate.

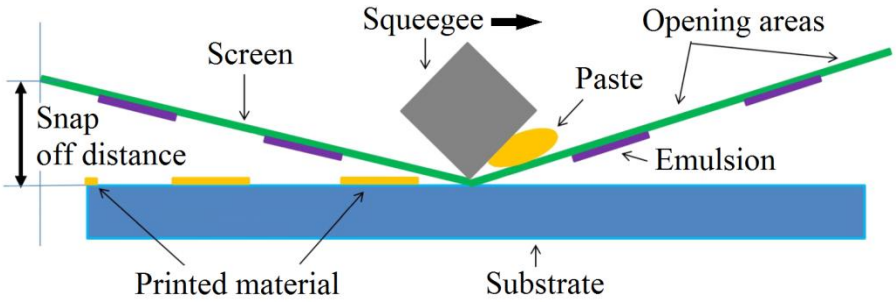

Figure 9 Scheme of the screen printing principle and the equipment involved

Applications of the screen printing in organic electronics include studies done by Bao et al. [61], who have manufactured the first full screen printed organic field-effect transistor. They have found an appropriate organic semiconductor for solution processing, poly-(3-hexylthiophene) (P3HT), and have built on the work of Garnier et al. [62]. The results showed that the

characteristics of the films involved were the same as those of spin-coated or cast films. The hole-transfer layer in OLEDs (organic light emitting diodes) has also been fabricated using screen printing technique by Jabbour et al. [63]. Screen printing of highly conductive PEDOT:PSS as an active layer or as conductive electrodes was done by several authors. They all proved that screen printing might be a suitable patterning method for PEDOT:PSS.

4.3 PHOTOLITHOGRAPHY

Photolithography (optical lithography or UV lithography) is a method used in microfabrication to pattern sections of a substrate. The fundamental concept behind photolithography is the selective exposure of a photosensitive polymer (photoresist), to ultraviolet light. Illumination of the photoresist through a mask leads to its selective exposure. The mask is usually made from opaque chrome feature on transparent quartz glass, or it can be a foil with precisely printed black patter for less demanding applications.

The exposed parts of the photoresist to the UV light results in the localized chemical reactions which take place within the photoresist and changes its solubility and creates distinct photoresist features. Photoresists are classified as either negative or positive, which depends on their solubility being either increased or decreased by optical exposure, respectively. Photoresists are usually processed in a liquid form, which is accomplished by the addition of solvents, and are coated as thin films onto suitable substrates by means of spin coating. During spin coating, the centrifugal forces exerted by a spinning substrate reduce its thickness to a proportional amount of spin speed and viscosity. Thicknesses ranging from tens of nanometers to hundreds of microns are routinely obtainable [57].

5 RESULTS AND DISCUSION

In this section, all the inkjet printing, screen printing and lithographic processes that were developed in our lab are listed together with detailed preparation procedures and measured results.

5.1 INKJET PRITENTED 24-WELL MICROPLATE

SensoPlate™ is a sterile microplate without bottom containing 24 wells with a flattened, raised ring to reduce cross-contamination, chimney well with alphanumeric coding made out of polystyrene. These platforms were used as templates for the development of OECT sensors. Microplates are routinely used for single molecule detection, fluorescence correlation spectroscopy, and confocal microscopy. SensoPlate™ has high optical clarity, low auto-fluorescence, and standard plate geometry – ANSI/SBS Standards (127.76 x 85.48 mm) with working volume per well of 0.5 to 1.5 ml (Figure 10). Micropaltes were purchased from Greiner Bio-One® (Greiner Bio-One North America Inc., Monroe, North Carolina, USA). Our goal was to print one OECT sensor into each well. Our prototypes made using inkjet printing and screen printing were developed to mount into these microplates and are described in the following chapters.

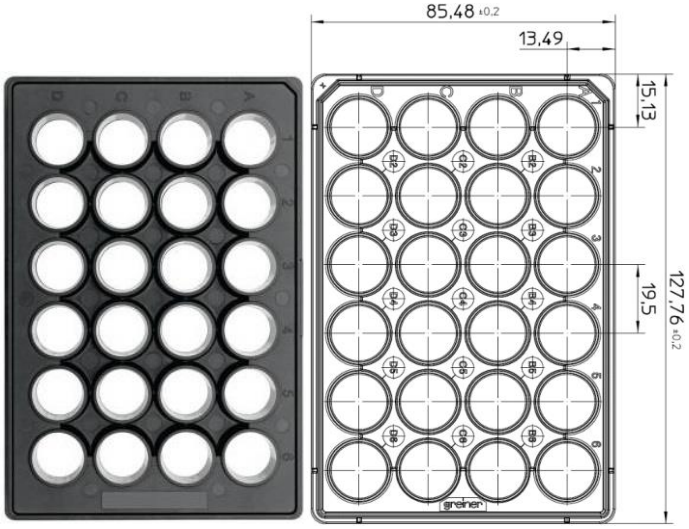

Figure 10 SensorPlate™ microplate with 24 wells, all dimensions are in mm

5.1.1 Fabrication

Inkjet printing of conductive and semiconductive layers was the necessary task to perform in order to manufacture the first prototypes of OECTs. Firstly, several versions of all planar OECT motives were designed. Then a matrix of 24 devices was put together to fit into the SensoPlate™ (Figure 11). First prototypes employed simple electrode system printed using silver ink and a semiconductive part printed with PEDOT:PSS.

In this section, for each ink, the general manufacturing process and a description of the printing is described. The optimization processes needed to produce functional devices have been presented in this chapter too.

The first OECT prototypes were designed to have channel dimensions of 1 cm x 500 μm. The gate electrode with dimensions of 1 cm x 2 mm was set 500 μm apart from the channel (Figure 11 Left). Patterns were designed with AutoCAD and subsequently converted to bitmaps with the

required resolution. Both the channel and gate electrode were inkjet-printed with PEDOT:PSS. Circuits printed out of the silver ink were placed outside of the cell cultivation area sealed by the silicone elastomer to avoid contact with the PBS and cells. The circuitry was terminated with five contacts compatible with standard connectors (Figure 11 Right). Transparent and flexible 150 µm thick PET foil was used as a substrate. Prior to the usage of the substrate, the cleaning by the two consecutive ultrasonic bath treatments (15 min each) first in Neodisher® LM3 surfactant (Chemische Fabrik Dr. Weigert GmbH & Co., Muhlenhagen, Germany), and then in deionized water was performed.

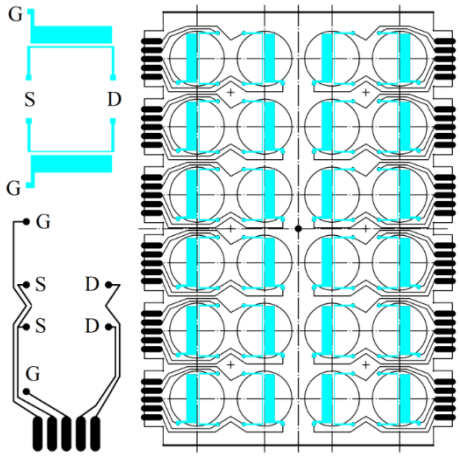

Figure 11 Designed patterns used to print 24 OECT arrays. Left: Close up of printing design of individual OECT sensors. Right: Envisioned 24 array layouts

5.1.2 Results and drawbacks

Resulting platform as shown in (Figure 12) consisted of 24 sensors that were mounted on SensoPlate™ and connected in sets of two to the measurement equipment. Each well was sealed from the top using rubber plugs in order to prevent drying of the electrolyte (PBS) from sensors during prolonged measurements.

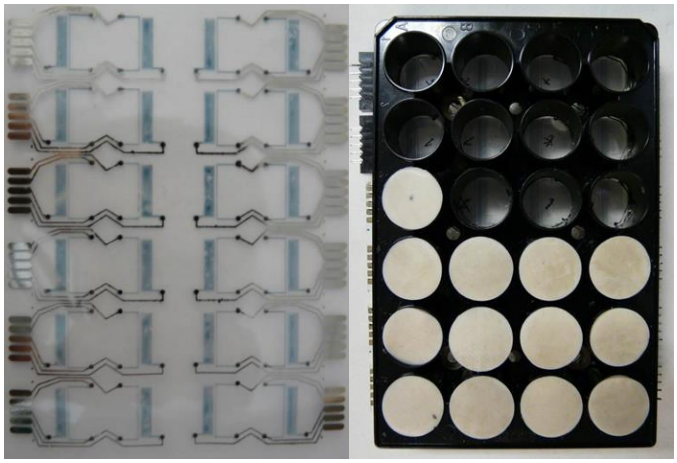

Figure 12 Left) Entirely inkjet printed matrix of 24 OECT sensors on transparent and flexible substrate. Right) Assembled SensoPlate™ with a rubber plug to minimize electrolyte evaporation

During the production of a fully inkjet-printed matrix of 24 sensors, we found few shortcomings in our design. Firstly, the PET substrates had insufficient thermal stability and during necessary thermal annealing at 150 °C (silver ink annealing) and even at 125 °C (PEDOT:PSS annealing) softened, waved and changed dimensions slightly.

The silver ink had to be printed on a surfactant treated substrate to achieve a good printing resolution, prevent unwanted ink spreading and pattern joining. Moreover, the silver layer had poor adhesion to the surface and had a tendency to swell and peel off after soaking in water or electrolyte. Furthermore, to print the compact active layer of PEDOT:PSS the substrate with printed silver ink circuits had to be plasma treated to modify surface energy. The process of the fully inkjet-printed matrix of 24 sensors was technologically demanding and lengthy, mainly due to the fact that the reliability of the print was poor. This was caused by the clogging of the nozzles during PEDOT:PSS printing. Moreover, a large number of misprinted samples due to the poor alignment of a substrate in the multi-layer device were caused by substrates dimensional changes.

5.2 SCREEN PRINTED 24-WELL MICROPLATE

In order to overcome the previously mentioned shortcomings, we used different printing technology, namely screen printing. Printing of the whole 24-well OECT matrix had proved to be a much faster and more reliable using screen printing method in comparison to inkjet printing. All screen printed layers had better adhesion to substrates and better reproducibility than inkjet-printed ones. Screen printing meshes with our own design were custom made (SERVIS CENTRUM a.s., Brno, Czech Republic). Layers of specific materials (screen printing pastes) were designed in three different iterations. First two designs (Figure 13) were very similar to previously used inkjet printing design and only differed in the PEDOT:PSS channel dimensions.

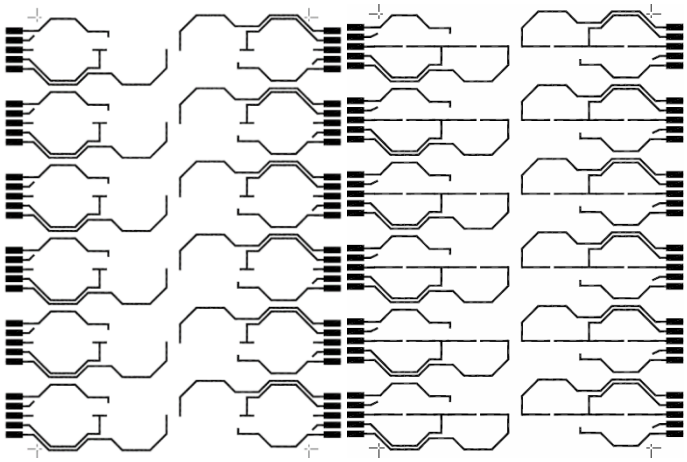

Figure 13 Left) Screen printed design with longer PEDOT:PSS channel (1 cm). Right) Screen printed design with shorter PEDOT:PSS channel (1 mm)

As a next step, we designed and manufactured a circular pattern with a better than before *Wd/L* ratio. In this case, we had to print one additional layer of silicone elastomer Sylgard® 184 to cover all silver/carbon circuitry (Figure 14 Right).

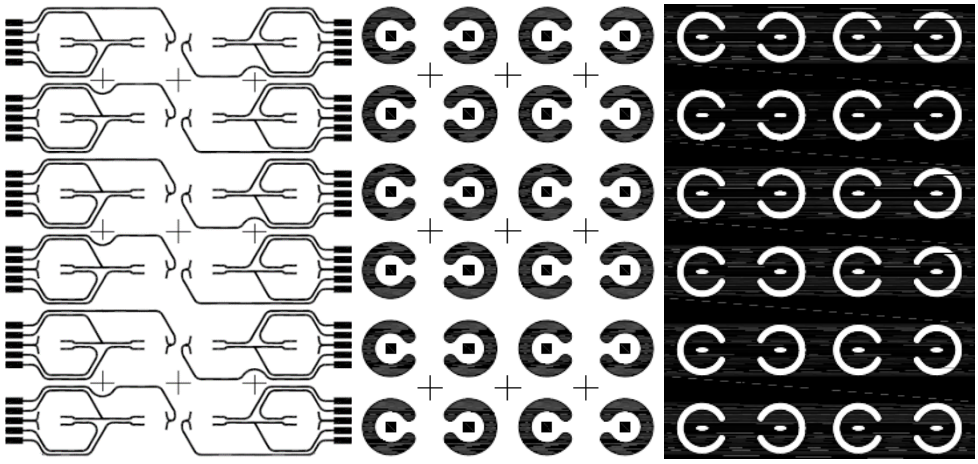

Figure 14 The screen printing pattern of silver circuit layer. Middle) The screen printing pattern of PEDOT:PSS gate and channel. Right) The screen printing pattern of covering layer of silicone elastomer Sylgard® 184

5.2.1 Fabrication

At first, it was necessary to prepare a substrate of the correct shape and to modify its surface properties. Polyethylene naphthalate (PEN) of 30 cm width and thickness of 250 μm (Goodfellow Cambridge Ltd., Huntingdon, UK) was used as a substrate. This was subsequently cut into the final shape compatible with the other parts of the sensor. The cut substrate was cleaned with a series of three ultrasonic baths, each of them lasting for 15 min. The first bath contained distilled water with a Neodisher® LM3 surfactant (Chemische Fabrik Dr. Weigert GmbH & Co., Muhlenhagen, Germany), the second bath contained distilled water and the last bath isopropyl alcohol.

5.2.2 Conductive pathways

The layer of silver conductive paste CB115v2 (DuPont Photopolymer and Electronic Materials, Wilmington, DE, USA) was printed onto a precisely positioned substrate (screen mesh count 77 threads/cm). It created the conductive contact with the paths that were 500 μm in width. The substrate with printed silver circuits was set to sinter at 120 °C on a heated pad for approximately 30 min. After curing the silver lines, the substrate was again aligned to print pattern of the semiconducting material. Other two conductive pastes: Flexible Silver Paste C2131014D3 and Heat Curable Carbon Paste C2050503P1 (Gwent Electronic Materials Ltd, Pontypool, UK) were used following the exact procedure as the CB115v2 paste.

5.2.3 Clevios™ S V3

The PEDOT:PSS layer was printed from commercially available Clevios™ S V3 screen printing pastes (Heraeus GmbH & Co. KG, Hanau, Germany). This paste performed the best from above-mentioned variants in terms of the quality of the print, although it had slightly worse conductivity in comparison to Clevios™ S V4. A detailed study of the influence of the printing parameters on the resulting sheet resistance and the homogeneity of the layers has been given in our previous work [64].

The PEDOT:PSS pattern was printed using a screen mesh count of 140 threads/cm and created a functional OECT gate and channel. The channel dimensions were 5 x 5 mm and the gate

electrode was produced by printing a semi-circle that opens on the one side for source and drain contacts.

5.2.4 Sylgard 184®

The device was masked and sealed by the third pattern of the silicone elastomer insulation layer, Sylgard® 184. The silicone elastomer was printed using screens with a mesh count of 120 threads/cm) and insulates the silver conducting paths from the electrolyte environment. It also prevents the tested biomaterial from coming into contact with the non-biocompatible parts and layers of the device. The silicone elastomer was mixed with the initiating agent at a ratio of 10:1 prior to printing. After that, it was printed on the re-aligned substrate and left to polymerize at room temperature for at least 24 h.

5.2.5 Characteristics of 24-well microplate

Screen print of both the organic semiconductor PEDOT:PSS ink as well as silver conducting paste resulted in reliable operating procedure and final function devices. The main characteristics of OECTs, the transconductance g = 100 μS and the time constant τ = 0.07 s at zero gate bias V_G = 0 V and 50 mV input gate signal were achieved.

5.3 SCREEN PRINTED 96 WELL MICROPLATE

SensoPlate™ with 96 wells was used as a template for the development of miniaturized OECT sensors. These microplates had standard plate geometry – ANSI/SBS Standards (127.76 x 85.48 mm) with working volume per well of 25 to 340 μl (Figure 15). It was purchased from Greiner Bio-One® (Greiner Bio-One North America Inc., Monroe, North Carolina, USA). Our goal was again to print one OECT sensor into each well. Prototypes were all made using screen printing and also photolithographic methods were developed, and are described in the following chapters. Reliability of devices was dependent on how well the individual layers adhere to the substrate and how they are able to resist in the long term. The reproducibility of the electrical properties of the individual sensors depends on the quality of printing and the ability to print all layers with the highest resolution possible. This is especially true in case of semiconductive material, which has to be as homogenously thick/thin as possible.

The aim of our research at this point was to prepare sensors that are functional, reliable, and have all more or less the same electrical properties. Previous experience with inkjet printing and screen printing of a 24-well microplate has shown that the functionality of sensors is primarily dependent on the continuity of all printed parts and proper multi-layer alignment. The significance of the thickness homogeneity of the PEDOT: PSS layer results from the OECT function. Since the OECT function is influenced by the injection of cations into the polymer layer and subsequent diffusion from the layer, it is important for the layer to have a uniform thickness. The thin parts of the layer would result in faster de-doping, while the thicker parts would still have highly conductive areas in the vicinity of the substrate.

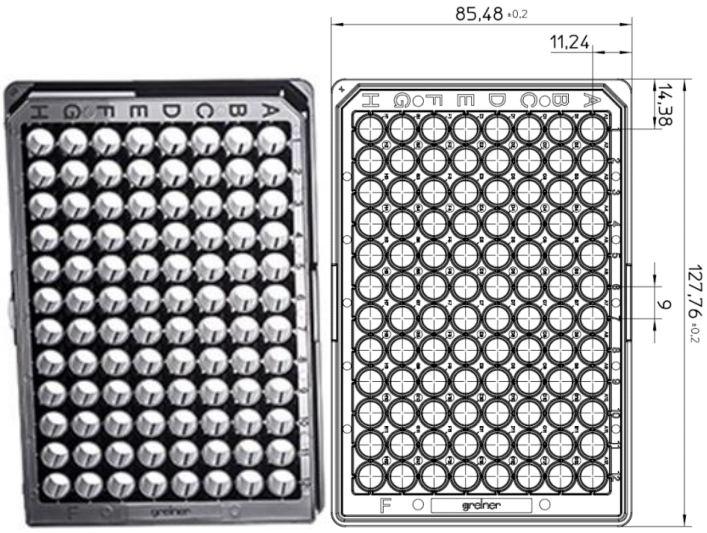

Figure 15 SensorPlate™ microplate with 96-wells, all dimensions are in mm

5.3.1 Fabrication

The fabrication of screen printed devices consisted of a series of processes adjusting the physical and chemical properties of both the surface of the substrate and also the printing pastes. The overall process was divided into several sub-steps, the order of which was experimentally determined and fixed. Replacing the order of these steps, or omitting one or more of them, would result in a faulty sensor. In this chapter, an extended summary of the fabrication process is given. The detailed fabrication steps and necessary printing adjustment are summed up in previous work [65].

At first, it was necessary to prepare a substrate of the correct shape and to modify its surface properties. Polyethylene naphthalate (PEN) of 30 cm width and thickness of 250 μm (Goodfellow Cambridge Ltd., Huntingdon, UK) was used as a substrate. This was subsequently cut into the final shape compatible with the other parts of the sensor. The cut substrate was cleaned with a series of three ultrasonic baths as detailed previously in the 24-well microplate section. All screen printing meshes with our own design were again custom made (SERVIS CENTRUM a.s., Brno, Czech Republic). Layers of specific materials (screen printing pastes) were printed on the cleaned substrate using designed patterns adjusted for a 96-well platform (Figure 16).

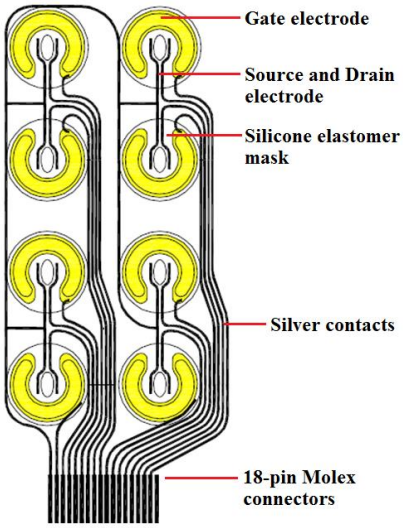

Figure 16 Detail of the printing patterns of 96-well platform

5.3.2 Silver conductive paste CB115v2

Firstly, the layer of silver conductive paste CB115v2 (DuPont Photopolymer and Electronic Materials, Wilmington, DE, USA) was printed onto a precisely positioned substrate (screen mesh count 77 threads/cm). That created a conductive field and the paths with a width of 180 μm. The substrate with printed silver circuits was set to sinter at 120 °C on a heated pad for approximately 30 min. After curing the silver lines, the substrate was again aligned to print pattern of the semiconducting material.

5.3.3 Clevios™ S V3

The PEDOT: PSS layer was printed from commercially available Clevios™ S V3 screen printing pastes (Heraeus GmbH & Co. KG, Hanau, Germany). The PEDOT:PSS pattern was printed using a screen mesh count of 140 threads/cm and created a functional OECT gate and channel. The channel dimensions were 1.5 x 1.5 mm, and the gate electrode was created by printing a semi-circle opened on the one side for source and drain contacts. The substrate with the printed layer was then placed on a heated pad at 120 °C for approximately 30 min until the layer had dried.

The paste was first stirred intensively before printing in order to obtain a lower viscosity and better homogeneity of the resulting film. AN ARG2 rheometer (TA Instruments, New Castle, DE, USA) was used for viscosity measurement at various shear rates at the fixed temperature of 25 °C. The PEDOT:PSS paste of gel consistency exhibited thixotropic behaviour. The static viscosity (at shear rates of 0.1/s) fell from the initial value above 1000 Pa·s down to as low as 15 Pa·s. This was achieved after several days of intensive stirring in a magnetic stirrer at laboratory temperature.

Additionally the stirring of the PEDOT:PSS Clevios™ S V3 was done in magnetic stirrer in a vial at 1000 rpm at elevated temperature of 90 °C. Typical curve depicted in (Figure 17) was obtained for given times of stirring. The stirring at ambient temperature resulted in the rapid change in viscosity that occurred after about 100 h of prior stirring.

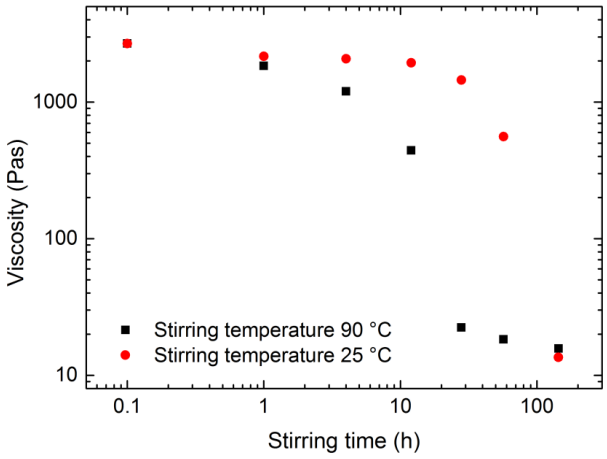

Figure 17 Effect of stirring at an ambient and elevated temperature on viscosity of PEDOT:PSS paste

The stirring at elevated temperature 90 °C shortened the time needed for this change to occur to 24 hours. The viscosity did not decrease further by additional stirring. The viscosity of the paste returned to the initial value in a matter of several hours after the stirring was stopped. Therefore, the printing had to be performed within a few minutes after stirring. Otherwise, the consistency of the paste returned to its initial gel state.

The stirring slightly decreased the resulting thickness of the layer by an average of 20 %, from 250 nm to 200 nm. It also improved the thickness homogeneity and roughness from 25 nm to 18 nm and waviness from 25 nm to 10 nm. These parameters were measured by a DektakXT Stylus Profiler (Bruker, Billerica, MA, USA).

Additionally, the sheet resistance decreased significantly from around 1 kΩ/square to 400 Ω/square. It is considered that intensive stirring acts similarly to alcohol treatment. Furthermore, the core-shell molecular structure changes in a linear fashion as was already reported, and the process is reversible [66]. This can also explain the resistance, roughness, and waviness reduction.

5.3.4 Sylgard 184

The system was masked and sealed by the third pattern of the silicone elastomer insulation layer, Sylgard® 184. The silicone elastomer was printed using screens with a mesh count of 120 threads/cm. This insulates the silver conducting paths from the electrolyte environment and also prevents the tested biomaterial from coming into contact with the non-biocompatible parts of the device. Sylgard ® 184 and every other component and material were tested for biocompatibility by the Institute of the Biophysics of the Czech Academy of Sciences [67].

The silicone elastomer was allowed to react at room temperature for 1 h after being thoroughly mixed with the initiating agent at a ratio of 10:1 prior to printing. After that, the silicone elastomer was printed on the re-aligned substrate. The silicone elastomer pattern was left to polymerize at 60 °C for at least 8 hours before further manipulation. The following screen print has provided a layer of the thickness of 12 µm. A coating to increase biocompatibility was done with Mouse Collagen, Type IV (BD Biosciences, cat. No. 354233), at 10 $\mu g \cdot cm^{-2}$ [68].

The detail of the sensor with labels S and D indicating the source and drain electrode, and the circular gate electrode G, all made out of PEDOT:PSS is depicted in (Figure 18). The OECT channel visible in (Figure 18), created by a screen-printed rectangular PEDOT:PSS layer on PEN foil, was surrounded by planar circular gate electrode 6 mm in outer diameter. The rotary symmetry should improve the electric field distribution. The electrodes were joined by printed silver conductors 0.2 mm wide. The printed transparent silicone layer covered the surface of the sensing array except for functional PEDOT:PSS interface with the biomaterial and physiological solution. The exposed channel area had length of $L = 1$ mm and width of $W = 1.5$ mm, the thickness of the PEDOT:PSS layer was 250 nm on average, and the typical electrical resistance of the channel was 500–700 Ω [65].

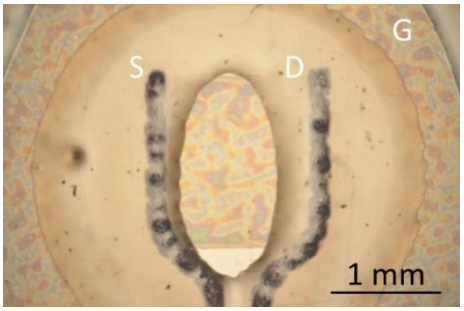

Figure 18 A detailed picture of one screen printed sensor. (S) Source electrode, (D) Drain electrode, (G) Gate electrode

5.3.5 Amplifier and measurement setup

The connect array of the microplate foil was connected by 18-pin Molex connectors and 18-wire ribbon conductors. Eight OECTs were connected by a single connector and each individual OECT could be selected from the array by a proper couple of micro-switches as shown in (Figure 19). Contrary to the majority of researchers, we used the planar arrangement of the electrodes for an easy optical and camera investigation [68].

The gate potential V_G was set from the external source in a range from −0.8 V to 0.8 V to prevent redox reactions at electrodes. Source and drain voltage V_D could be set down to −0.725 V. The source current I_S was converted to voltage in an I/V converter and recorded by an oscilloscope after further amplification. The offset I_S at a stable working point was compensated by setting the corresponding opposite current at the input of the operating amplifier. The zero Analog OUT voltage was set as an input voltage of $V_G = 0$ V via R_{offset} resistor/potentiometer. The feedback resistor $R_{sense} = 1$ kΩ gives a conversion of 1 mA/1 V. Further amplification was enabled by switching the output jumper [68].

The electric field strength at the channel vicinity determined the effective ion drift through the channel and consequently the channel conductance. The small channel area at the interface with the electrolyte compared with the large gate electrode area enhanced the electric field. Together with the volumetric capacitance of OECT, it was responsible for the device amplification and speed. The capacitance of the electrode in a physiological solution of phosphate-buffered saline (PBS) based on a 0.15 M solution of NaCl was estimated at $C = 0.2$ F·mm^{-2}.

Together with the electrolyte conductance of $g = 1$ μS, the time constant $t = 0.2$ s was anticipated. The capacitance of the much larger gate electrode could be neglected due to its serial combination with the channel capacitance. The speed of the OECT device was limited by the

capacitance of the gate circuit. It was controlled by the effective capacitance of the channel. The label ‘effective’ here takes into account that the potential at the channel is not uniform but distributed non–linearly along its length from the source to the drain electrode (from 0 to −0.725 V in our case). It was, to some degree, considered a consequence of the channel aspect–ratio. Moreover, the geometry of the entire system including the gate electrode and electrolyte could influence the channel potential distribution.

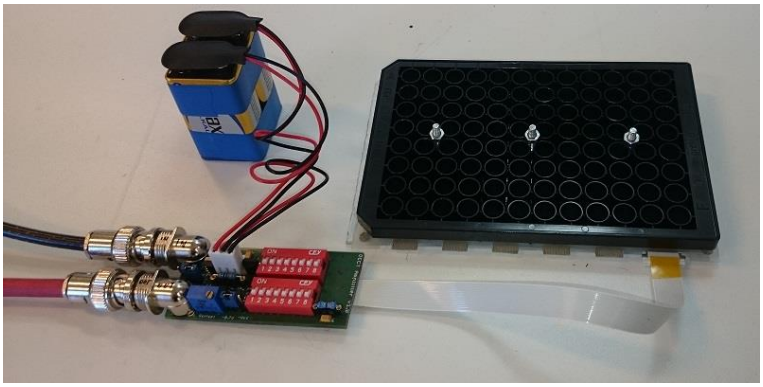

Figure 19 Encapsulated OECT – 96 well microplate with a power source-signal amplifier and current/voltage converter

The gate offset voltage as well the voltage modulation (simulation of the cardiomyocyte pulsing), were delivered from the function generator to the Analog IN input. An OECT was selected by a couple of switches as shown in (Figure 19). The drain was supplied by a negative voltage down to $V_D = -0.735$ V. This value was set due to the factory setting. It represented a compromise between the requirement of a safety voltage against electrode redox reactions in the event of a positive gate voltage ($V_G > 0$ V) and the necessity of high amplification (transconductance g). Its fixed value enabled comparing the amplification of OECT devices at any point in time. The source was connected to a virtual zero input of the *I/V* converter. The amplified signal was recorded by a digital memory oscilloscope. The offset of the stable channel current was compensated for by a potentiometer R_{offset} so the Analog OUT DC signal component could be eliminated [68].

5.3.6 Results

The first experiment tested the OECT parameters such as the transfer characteristics and the derived transconductance g. The fix drain potential was set to $V_D = -0.735$ V, and the output source current was measured continuously at the triangular, symmetric gate voltage V_G in a range of 0.2 to −0.8 V. The results can be found in (Figure 20). The transfer characteristics in our case show significant hysteresis. In the case of a short period of about $T = 1$ s, the volumetric capacitance charging delays the output current I_S, so the hysteresis is oriented counter-clockwise. In the case of a long period of $T = 20$ s, slow relaxations of the polymer network in the channel, reducing the output current I_S, dominate so that the hysteresis is oriented clockwise. In the case of a medium period of $T = 5$ s, both effects are compensated.

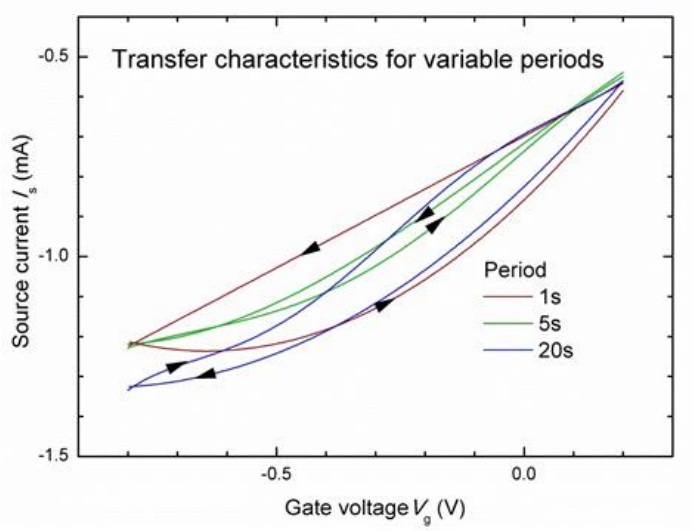

Figure 20 Transfer characteristics measured at the triangular gate periodic voltage at various periods [68]

The second experiment, investigating the response of an OECT's channel current on a simulated signal of electrogenic cells, was conducted (Figure 20). The standard PBS solution was used as an electrolyte. In looking for the optimum working point of the OECT with the highest transconductance, the gate voltage V_G from the function generator was modulated by rectangular pulses of 10 mV_{pp} at a 5 s period.

The aging of the OECT structure under the voltage load described above was performed over a period of 28 h (Figure 21). A gradual, approximately 25 % decrease of I_S and the transconductance g was recorded.

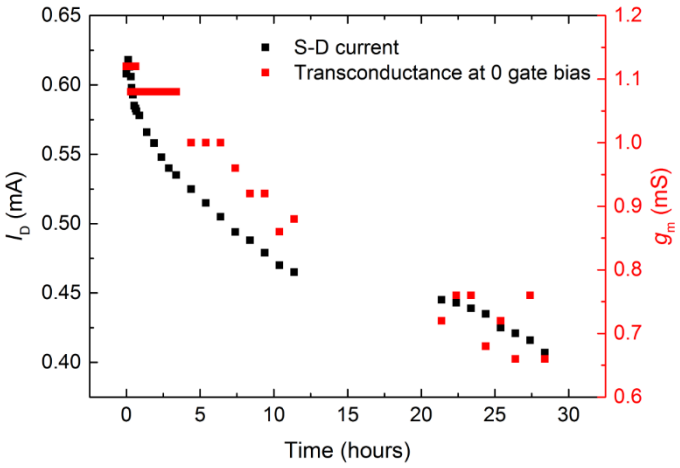

Figure 21 OECT degradation at $V_D = -0.735$ V and $V_G = 0$ V in PBS solution

The biocompatibility of the sensor was tested by 3T3 fibroblasts. Cells were able to grow on sensors to the same extent as on control substrates (standard cell culture plastics). The cell viability was comparable to that of control substrates, and it typically reached 90 – 95 %. This indicated that a high level of biocompatibility was reached. Indeed cells were able to form a confluent layer within 48 h (Figure 22 A). A proof of concept experiment for the sensor function was carried out.

Due to extensive ion exchange, the cells grown at the transistor channel modulate the current within it. Therefore the removal of cells resulted in changes in the channel current. Thus, the confluent layer of cells within the sensor was treated with trypsin, an approach to detach cells from their support [68]. Indeed, the absolute value of the current decreased in parallel to the trypsin-mediated detachment of cells (Figure 22 B).

Finally, the function of the sensor was verified through a spike of KCl (Lachema, Brno, Czech Republic), which resulted in a significant dropdown of the absolute current value. The main idea of the final proof of concept experiment with cells was to demonstrate that the sensor can host the living cells efficiently and an electrogenic event related to cell physiology could be recorded.

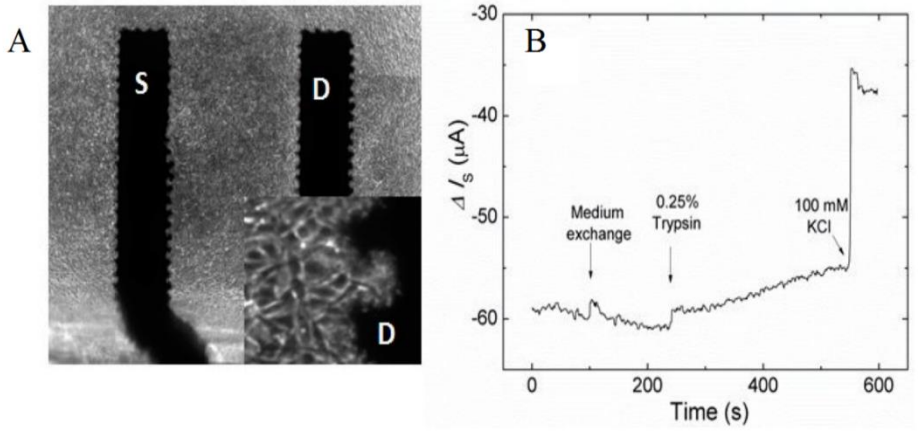

Figure 22 (A) OECT with a confluent layer of 3T3 fibroblasts: S – source, D – drain (B) The electrical response to cell release due to trypsin. 100 mM KCl spike served as a positive control of transistor function [68]

5.4 SU-8 PHOTOLITHOGRAPHY

In good agreement with previously published works improvement of the transconductance and time constant of prepared devices can be achieved by decreasing the OECT dimensions [69]. The increase in parameters mentioned above is done by shortening the gate-channel distance and minimizing the channel-electrolyte volumetric capacitance by reducing the channel area. The miniaturization and optimization were done via photolithography using SU-8 photoresist.

5.4.1 Fabrication process

The combination of photolithographic techniques together with screen-printing method was employed for the device assembly. The copper laminates on a PEN-film backing with a thickness of 50 μm (AKAFLEX PENCL HT provided by Gatema a.s, Boskovice, Czech Republic), was used to photolithographically pattern flexible circuits. The PEN variant was chosen due to its superior stability at high temperatures compared to PET laminates and enabled processing at a temperature of up to 150 °C. On top of the patterned electrolytic copper foil (thickness of 17 μm) was galvanically applied a thin layer of gold (10–100 nm) with an interlayer of nickel for better adhesion. The PEDOT:PSS layer was printed from commercially available Clevios™ S V3 screen printing pastes (Heraeus GmbH & Co. KG, Hanau, Germany). The PEDOT:PSS pattern created a functional OECT gate and channel. PEDOT:PSS was screen-printed in the form of a rectangular channel connecting two parallel gold electrodes with a width of 250 μm and 200 μm gap between

them. The channel was surrounded by a planar circular gate electrode also printed using PEDOT:PSS with an outer diameter of 6 mm (Figure 23).

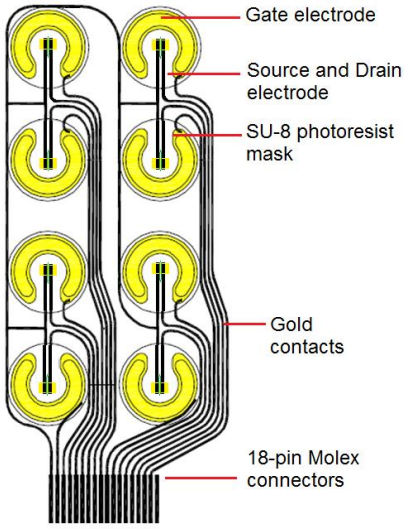

Figure 23 The detail of the designed OECT array

5.4.2 Screen printing of SU-8

The device was sealed by the layer of photoresist SU-8 (MicroChem Corp. Westborough, MA, USA). This layer insulated the gold conducting paths from the electrolyte environment and created a narrow active channel.

For screen printing the RokuPrint Screen printing machine, SD 05 was used together with custom-made polyethylene screens 36/31 (36 µm – size of mesh opening, 31 µm – the size of thread diameter) for screen printing of Clevios S V3 PEDOT:PSS and 140/65 screen for screen printing of SU-8 photoresist. The layers of approximately 200 nm of PEDOT: PSS and 30 µm of SU-8 were obtained. To this end, the SU-8 2015 with a viscosity of 1250 cSt had to be diluted by cyclopentanone to the viscosity of approximately 250 cSt. An ARG2 rheometer (TA Instruments, New Castle, DE, USA) was used for viscosity measurement at the fixed temperature of 25 °C.

The prepared screen-printed layer was firstly dried on a hot plate at 95 °C for 5 min (soft bake). This step was necessary in order to minimize the amount of solvent in the layer of SU-8 before exposure. The resulting photoresist layer was 30 µm thick. The unexposed photoresist substrate was then aligned under a microscope with a chrome photomask made by electron-beam lithography and placed in the Suss Microtech MA6/BA6 adjuster (Institute of Scientific Instruments, The Czech Academy of Sciences, Brno). The photoresist was exposed to UV radiation of 5.6 mW/cm^2 for 120 s. This step was followed by another heat curring on a hot plate for 5 min at 100 °C (post exposure bake). This step was necessary for the development of the desired pattern. Subsequently, the photoresist was submerged for 1 min in the developer, rinsed with isopropyl alcohol and dried in nitrogen flow.

The screen printed and the photolithographically patterned layer of SU-8 covers the surface of the whole OECT sensing array as can be seen in (Figure 24).

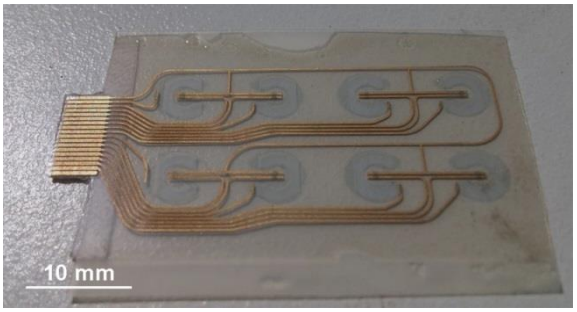

Figure 24 Screen-ptinted and photolithographically patterned OECT sensor array

Only parts of the sensor that comes in contact with the electrolyte (active channel and gate electrode) are exposed. The exposed channel area had the dimension of $L = 50$ µm and a width of $W = 600$ µm as shown in (Figure 25). The typical electrical resistance of the channel was 200–300 Ω.

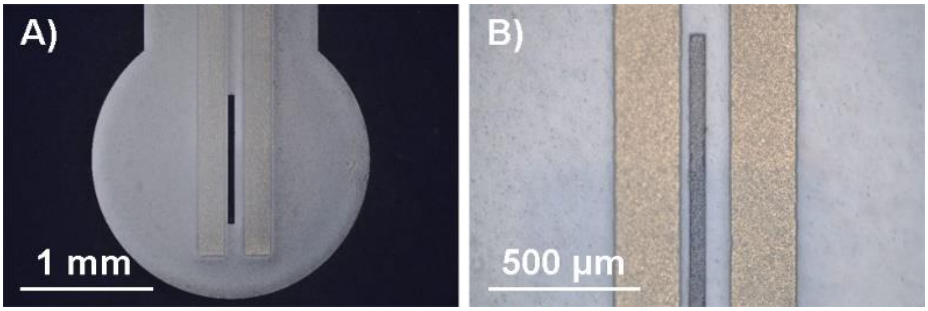

Figure 25 The detail of one sensor channel patterned using SU-8 photoresist

The electrical circuitry designed for OECT remained the same as previously. The connector array at the microplate foil was contacted by 18-pin Molex connectors and 18-wire ribbon conductors so that a single connector connected eight OECTs. Individual OECT could be selected from the array by a proper couple of microswitches.

5.4.3 Results

The initial test determined the OECTs parameters such as output characteristics (Figure 26) and transfer characteristics (Figure 27), and from them, the highest derived transconductance $g = 2.5$ mS which was comparable or even better than state of the art fully lithographically prepared devices. The next experiment investigated the response of an OECT's channel current on a simulated signal of electrogenic cells. The standard PBS solution was used as an electrolyte. In looking for the optimum working point of the OECT with the highest transconductance, the gate voltage V_G was set to 0.2 V and the voltage between Source and Drain electrode was set to $V_D = -0.4$ V. The rectangular pulses of 1 mV_{pp} at a 1 s period were modulated. Typical response on such pulse together with filtered data using FFT (fast Fourier transform) bandpass from 0 to 25 Hz and determined value of the time constant can be seen in (Figure 28).

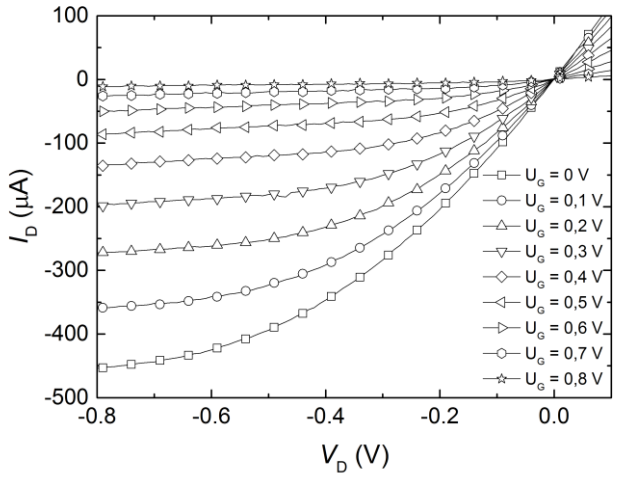

Figure 26 Output characteristics of 96-well OECT with SU-8 as covering layer

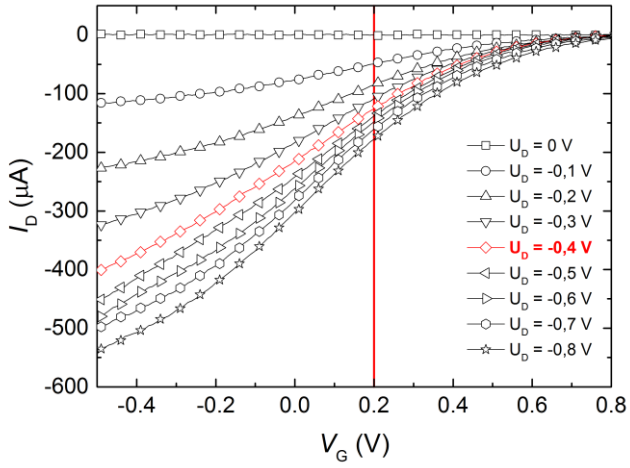

Figure 27 Transfer characteristics with the illustration of set point and the slope dependent on the drain potential

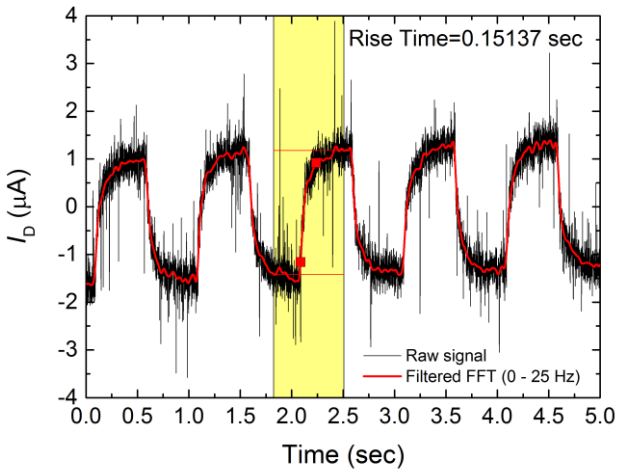

Figure 28 Response of OECT to 1 mV_{pp} gate rectangular signal at setting point $V_D = -0.4$ V, $V_G = 0.2$ V

The screen printing process of commercially available and biocompatible photoresist SU-8 was optimized and successfully implemented into previously adapted OECT sensors based on PEDOT:PSS. Using the photolithographic process the pattern of 50 mm thin active channel was achieved. Signal amplification was shown employing an electrogenic cell pulsation simulation, where the constant gate offset potential was modulated by a 1.0 Hz, 1.0 mV_{pp} rectangular signal. The resulting Source-Drain current response I_D was 2.5 µA, and the corresponding achieved transconductance 2.5 mS. The upper-frequency limit 7 Hz was concluded from the OECT gate circuit time constant of 0.15 s.

6 CONCLUSION

The main goal of this dissertation thesis was to compile a comprehensive overview of organic electrochemical transistors, fabrication of such a device using conventional printing techniques and their subsequent use as a bioelectronic sensor. The manufacturing process was done in several iterations consisting of multiple steps. Firstly the inkjet printing of conductive and semiconductive layers was the necessary task to perform in order to manufacture the very first prototypes of OECTs. Several versions of all planar OECT motives were designed to be mounted into a matrix of 24 devices of SensoPlate™. First prototypes employed simple electrode system printed using silver ink and a semiconductive PEDOT:PSS. The first OECT prototypes were designed to have channel dimensions of 1 cm x 500 μm. The gate electrode with dimensions of 1 cm x 2 mm was set 500 μm apart from the channel. Patterns were designed with Autodesk AutoCAD. Both the channel and gate electrode were inkjet-printed using PEDOT:PSS. Circuits printed out of silver ink were placed outside of the cell cultivation area sealed by the silicone elastomer Sylgard® 184 to prevent contact with the PBS and living cells. The circuitry was terminated with five contacts compatible with standard connectors. Transparent and flexible 150 μm thick PET foil was used as a substrate.

During the production of a fully inkjet-printed matrix of 24 sensors, we found out few shortcomings in our design. Firstly, the PET substrates had insufficient thermal stability and during necessary thermal annealing at 150 °C (silver ink annealing) and even at 125 °C (PEDOT:PSS annealing) softened, waved and changed dimensions slightly. The silver ink had to be printed on a surfactant treated substrate in order to achieve good printing resolution, prevent unwanted ink spreading and pattern joining. Moreover, the silver layer had poor adhesion to the surface and had a tendency to swell and peel off after soaking in water or electrolyte. Furthermore, to print the compact active layer of PEDOT:PSS the substrate with printed silver ink circuits had to be plasma treated to modify its surface energy. The process of the fully inkjet-printed matrix of 24 sensors was technologically demanding and lengthy, mainly due to the fact that the reliability of the prints was poor. This was aggravated by the constant clogging of the nozzles during PEDOT:PSS printing. On top of that, a large number of misprinted samples due to the poor alignment of a substrate in the multi-layer device were caused by substrates dimensional changes.

In order to overcome previous shortcomings, we used screen printing technology to print the whole 24-well OECT matrix. It had proved to be a much faster and more reliable technique. All screen printed layers had better adhesion to substrates and better reproducibility than inkjet-printed ones. Layers of specific materials were designed in three different iterations.

Previous experience with inkjet printing and screen printing of a 24-well microplate has shown that the functionality of sensors is primarily dependent on the continuity of all printed parts and proper multi-layer alignment. The significance of the thickness homogeneity of the PEDOT: PSS layer results from the OECT function. Since its function is influenced by the injection of cations into the polymer layer and subsequent diffusion from the layer, it is important for the layer to have a uniform thickness over its entire surface.

The homogeneity of the PEDOT:PSS was addressed by the intensive stirring of the paste. The stirring slightly decreased the resulting thickness of the layer by an average of 20 %, from 250 nm to 200 nm and also improved the thickness homogeneity and roughness from 25 nm to 18 nm and waviness from 25 nm to 10 nm.

The PEDOT:PSS paste of gel consistency exhibited thixotropic behaviour. The static viscosity after stirring fell from the initial value of above 1000 Pa·s down to as low as 15 Pa·s. This was

achieved after several days of intensive stirring in a magnetic stirrer at laboratory temperature or at an elevated temperature of (90 °C) in a matter of hours.

To further improve device performance we opted to decrease crucial OECT dimensions. That meant shortening the gate-channel distance and minimalizing the capacitance by reducing the channel area. To this end an all screen printed 96-well array of OECTs for cell culture electrical response monitoring was developed.

We also developed an electrical circuit designed for OECT testing with the connector array at the microplate foil connected by 18-pin Molex connectors and 18-wire ribbon conductors. In this way, the eight OECTs were connected by a single connector and individual OECTs could be selected from the array by a proper couple of micro-switches. The gate potential V_G was set from the external source in a range from −0.8 V to 0.8 V to prevent redox reactions at electrodes. Source and drain voltage V_D could be set down to −0.725 V. The source current I_S was converted to voltage in an *I*/*V* converter and recorded by an oscilloscope after further amplification.

Due to relaxations, the transfer characteristics and transconductance *g* included were strongly dependent on the sweep rate of the testing gate voltage V_G and its direction. The sharp transconductance maximum and its position at the V_G axis dependent on the channel geometry was reported in the literature, but no sweep rate influence was previously mentioned. The transfer characteristics also showed significant hysteresis.

To improve the biocompatibility of the PEDOT:PSS screen printing paste it was mixed with increasing concentration of Mouse Collagen, Type IV. Resulting composites were tested by the Institute of the Biophysics of the Czech Academy of Sciences. The cell viability was assessed by using MTT test and by the fluorescein diacetate and propidium iodide (FDA/PI) staining. All tests were done employing 3T3 fibroblasts using the 96-well platform.

To further miniaturize manufacturing process of OECT biosensor production based on PEDOT:PSS the screen printing process of commercially available and biocompatible photoresist SU-8 was optimized and successfully implemented. Using the photolithographic process the pattern of 50 mm thin active channel was achieved. Signal amplification was shown employing an electrogenic cell pulsation simulation, where the constant gate offset potential was modulated by a 1.0 Hz, 1.0 mV_{pp} rectangular signal. The resulting Source-Drain current response I_d was 2.5 μA, and the corresponding achieved transconductance of 2.5 mS. The upper-frequency limit 7 Hz was concluded from the OECT gate circuit time constant of 0.15 s.

3T3 fibroblasts were used to test the biocompatibility of the sensors. Cells were able to grow on top of the sensors to the same degree as in control substrates (standard cell culture plastics). The cell viability was similar to the control and was typically around 90 – 95 %. The unimpaired viability indicated that a high level of biocompatibility was reached.

To conclude, we were successfully able to produce microelectronic arrays of OECT sensors using standard printing techniques employing only commercially available materials. This approach is cheap, accessible and easy to implement during routine cell culture assessments. All our devices were manufactured without the need for cleanroom facilities, quickly, reliably and in large quantities. OECT sensors were biocompatible and able to measure the simulated response of the cardiac cells to the required extent.

7 LITERATURE

[1] MALLIARAS, George a Richard FRIEND. An organic electronics primer. *Physics Today* [online]. 2005, 58(5): 53-58 [cit. 2015-07-14]. DOI: 10.1063/1.1995748. ISSN 0031-9228.

[2] TARABELLA, Giuseppe, Gaurav NANDA, Marco VILLANI, Nicola COPPEDÈ, Roberto MOSCA, George G. MALLIARAS, Clara SANTATO, Salvatore IANNOTTA a Fabio CICOIRA. Organic electrochemical transistors monitoring micelle formation. *Chemical Science* [online]. 2012, 3(12): 3432- [cit. 2015-07-14]. DOI: 10.1039/c2sc21020g. ISSN 2041-6520.

[3] PEI, Q., G. YU, C. ZHANG, Y. YANG a A. J. HEEGER. Polymer Light-Emitting Electrochemical Cells. *Science* [online]. 1995, 269(5227): 1086-1088 [cit. 2015-07-14]. DOI: 10.1126/science.269.5227.1086. ISSN 0036-8075.

[4] MORTIMER, Roger J., Aubrey L. DYER a John R. REYNOLDS. Electrochromic organic and polymeric materials for display applications. *Displays* [online]. 2006, 27(1): 2-18 [cit. 2015-07-14]. DOI: 10.1016/j.displa.2005.03.003. ISSN 01419382.

[5] BERNARDS, D. A., S. FLORES-TORRES, H. D. ABRUNA a G. G. MALLIARAS. Observation of Electroluminescence and Photovoltaic Response in Ionic Junctions. *Science* [online]. 2006, 313(5792): 1416-1419 [cit. 2015-07-14]. DOI: 10.1126/science.1128145. ISSN 0036-8075.

[6] BERGGREN, M. a A. RICHTER-DAHLFORS. Organic Bioelectronics. *Advanced Materials* [online]. 2007, 19(20): 3201-3213 [cit. 2015-07-14]. DOI: 10.1002/adma.200700419. ISSN 09359648.

[7] SVENNERSTEN, Karl, Karin C. LARSSON, Magnus BERGGREN a Agneta RICHTER-DAHLFORS. Organic bioelectronics in nanomedicine. *Biochimica et Biophysica Acta (BBA) - General Subjects* [online]. 2011, 1810(3): 276-285 [cit. 2015-07-14]. DOI: 10.1016/j.bbagen.2010.10.001. ISSN 03044165.

[8] OWENS, Róisín, Peter KJALL, Agneta RICHTER-DAHLFORS a Fabio CICOIRA. Organic bioelectronics — Novel applications in biomedicine. *Biochimica et Biophysica Acta (BBA) - General Subjects* [online]. 2013, 1830(9) [cit. 2015-07-14]. DOI: 10.1016/j.bbagen.2013.04.025. ISSN 03044165.

[9] BUZSÁKI, György, Costas A. ANASTASSIOU a Christof KOCH. The origin of extracellular fields and currents — EEG, ECoG, LFP and spikes. *Nature Reviews Neuroscience* [online]. 2012-5-18, 13(6): 407-420 [cit. 2015-07-14]. DOI: 10.1038/nrn3241. ISSN 1471-003x.

[10] RIVNAY, Jonathan, Róisín M. OWENS a George G. MALLIARAS. The Rise of Organic Bioelectronics. *Chemistry of Materials* [online]. 2014, 26(1): 679-685 [cit. 2015-07-14]. DOI: 10.1021/cm4022003. ISSN 0897-4756.

[11] SCHUMACHER, Soeren, Jörg NESTLER, Thomas OTTO, Michael WEGENER, Eva EHRENTREICH-FÖRSTER, Dirk MICHEL, Kai WUNDERLICH, Silke PALZER, Kai SOHN, et al. Highly-integrated lab-on-chip system for point-of-care multiparameter analysis. *Lab Chip* [online]. 2012, 12(3): 464-473 [cit. 2015-07-14]. DOI: 10.1039/C1LC20693A. ISSN 1473-0197

[12] ROBINSON, Nathaniel D., Per-Olof SVENSSON, David NILSSON a Magnus BERGGREN. On the Current Saturation Observed in Electrochemical Polymer Transistors. *Journal of The Electrochemical Society* [online]. 2006, 153(3): H39- [cit. 2015-07-14]. DOI: 10.1149/1.2172534. ISSN 00134651.

[13] WHITE, Henry S., Gregg P. KITTLESEN a Mark S. WRIGHTON. Chemical derivatization of an array of three gold microelectrodes with polypyrrole: fabrication of a molecule-based transistor. *Journal of the American Chemical Society* [online]. 1984, 106(18): 5375-5377 [cit. 2015-07-24]. DOI: 10.1021/ja00330a070. ISSN 0002-7863.

[14] HEYWANG, Gerhard, Friedrich JONAS, Anja VAN DE STOLPE, Thomas MEYER, Robert PASSIER, Christine L. MUMMERY, M. C. SANGUINETTI a M. T. KEATING. *Poly(alkylenedioxythiophene)s—new, very stable conducting polymers* [online]. [cit. 2018-09-25]. DOI: 10.1002/adma.19920040213. ISBN 0935-9648. Dostupné z: http://doi.wiley.com/10.1002/adma.19920040213

[15] YAMATO, Hitoshi, Masaki OHWA, Wolfgang WERNET, Thomas MEYER, Robert PASSIER, Christine L. MUMMERY, M. C. SANGUINETTI a M. T. KEATING. *Stability of polypyrrole and poly(3,4-ethylenedioxythiophene) for biosensor application* [online]. [cit. 2018-09-25]. DOI: 10.1016/0022-0728(95)04156-8. ISBN 1572-6657. Dostupné z: http://linkinghub.elsevier.com/retrieve/pii/0022072895041568

[16] ELSCHNER, Andreas, Stephan KIRCHMEYER, Wilfried LOVENICH, Udo MERKER a Knud REUTER. *PEDOT: principles and applications of an intrinsically conductive polymer*. Boca Raton, FL: CRC Press, 2010. ISBN 978-142-0069-112.

[17] BERNARDS, D. A. a G. G. MALLIARAS. Steady-State and Transient Behavior of Organic Electrochemical Transistors. *Advanced Functional Materials* [online]. 2007, 17(17): 3538-3544 [cit. 2015-07-14]. DOI: 10.1002/adfm.200601239. ISSN 1616301x

[18] KHODAGHOLY, Dion, Jonathan RIVNAY, Michele SESSOLO, et al. High transconductance organic electrochemical transistors. *Nature Communications* [online]. 2013-7-12, 4, - [cit. 2016-02-03]. DOI: 10.1038/ncomms3133. ISSN 2041-1723.

[19] NIELSEN, Christian B., Alexander GIOVANNITTI, Dan-Tiberiu SBIRCEA, et al. *Molecular Design of Semiconducting Polymers for High-Performance Organic Electrochemical Transistors* [online]. [cit. 2018-09-25]. DOI: 10.1021/jacs.6b05280. ISBN 0002-7863.

[20] RIVNAY, Jonathan, Sahika INAL, Alberto SALLEO, et al. *Organic electrochemical transistors* [online]. [cit. 2018-09-26]. DOI: 10.1038/natrevmats.2017.86. ISBN 2058-8437.

[21] KHODAGHOLY, Dion, Thomas DOUBLET, Pascale QUILICHINI, et al. In vivo recordings of brain activity using organic transistors. *Nature Communications* [online]. 2013-3-12, 4, 1575- [cit. 2016-01-21]. DOI: 10.1038/ncomms2573. ISSN 2041-1723.

[22] RIVNAY, J., P. LELEUX, M. FERRO, et al. High-performance transistors for bioelectronics through tuning of channel thickness. *Science Advances* [online]. 2015, **1**(4), e1400251-e1400251 [cit. 2018-09-25]. DOI: 10.1126/sciadv.1400251. ISBN 0002-7863. ISSN 2375-2548.

[23] STRAKOSAS, Xenofon, Manuelle BONGO a Róisín M. OWENS. The organic electrochemical transistor for biological applications. *Journal of Applied Polymer Science* [online]. 2015, 132(15), n/a-n/a [cit. 2016-02-15]. DOI: 10.1002/app.41735. ISSN 00218995.

[24] LIN, Peng, Feng YAN, M. FERRO, et al. Organic Thin-Film Transistors for Chemical and Biological Sensing. *Science Advances* [online]. 2015, **1**(4), e1400251-e1400251 [cit. 2018-09-25]. DOI: 10.1002/adma.201103334. ISBN 0935-9648. ISSN 2375-2548.

[25] NILSSON, D., N. ROBINSON, M. BERGGREN, et al. Electrochemical Logic Circuits. *Science Advances* [online]. 2015, **1**(4), e1400251-e1400251 [cit. 2018-09-25]. DOI: 10.1002/adma.200401273. ISBN 0935-9648. ISSN 2375-2548. Dostupné z: http://doi.wiley.com/10.1002/adma.200401273

[26] HUTTER, Philipp C., Thomas ROTHLANDER, Gregor SCHEIPL, et al. All Screen-Printed Logic Gates Based on Organic Electrochemical Transistors. *Science Advances* [online]. 2015, **1**(4), e1400251-e1400251 [cit. 2018-09-25]. DOI: 10.1109/TED.2015.2491342. ISBN 0018-9383. ISSN 2375-2548.

[27] GKOUPIDENIS, Paschalis, Dimitrios A. KOUTSOURAS, George G. MALLIARAS, et al. Neuromorphic device architectures with global connectivity through electrolyte gating. *Science Advances* [online]. 2015, **1**(4), e1400251-e1400251 [cit. 2018-09-25]. DOI: 10.1038/ncomms15448. ISBN 2041-1723. ISSN 2375-2548.

[28] VAN DE BURGT, Yoeri, Ewout LUBBERMAN, Elliot J. FULLER, et al. *A non-volatile organic electrochemical device as a low-voltage artificial synapse for neuromorphic computing* [online]. [cit. 2018-09-26]. DOI: 10.1038/nmat4856. ISBN 1476-1122.

[29] BERGGREN, M., D. NILSSON a N. D. ROBINSON. *Organic materials for printed electronics* [online]. [cit. 2018-09-26]. DOI: 10.1038/nmat1817. ISBN 1476-1122.

[30] KAPHLE, Vikash, Shiyi LIU, Akram AL-SHADEEDI, Chang-Min KEUM a Björn LÜSSEM. *Contact Resistance Effects in Highly Doped Organic Electrochemical Transistors* [online]. [cit. 2018-09-26]. DOI: 10.1002/adma.201602125. ISBN 0935-9648.

[31] FRIEDLEIN, Jacob T., Jonathan RIVNAY, David H. DUNLAP, Iain MCCULLOCH, Sean E. SHAHEEN, Robert R. MCLEOD a George G. MALLIARAS. *Influence of disorder on transfer characteristics of organic electrochemical transistors* [online]. [cit. 2018-09-26]. DOI: 10.1063/1.4993776. ISBN 0003-6951.

[32] GIOVANNITTI, Alexander, Christian B. NIELSEN, Dan-Tiberiu SBIRCEA, et al. *N-type organic electrochemical transistors with stability in water* [online]. [cit. 2018-09-26]. DOI: 10.1038/ncomms13066. ISBN 2041-1723.

[33] GIOVANNITTI, Alexander, Dan-Tiberiu SBIRCEA, Sahika INAL, et al. *Controlling the mode of operation of organic transistors through side-chain engineering* [online]. [cit. 2018-09-26]. DOI: 10.1073/pnas.1608780113. ISBN 0027-8424.

[34] HÜTTER, Philipp C., Thomas ROTHLÄNDER, Anja HAASE, et al. *Influence of geometry variations on the response of organic electrochemical transistors* [online]. [cit. 2018-09-26]. DOI: 10.1063/1.4816781. ISBN 0003-6951.

[35] BARD, Allen J a Larry R FAULKNER. *Electrochemical methods: fundamentals and applications*. 2nd ed. New York: Wiley, c2001. ISBN 978-0-471-04372-0.

[36] KOUTSOURAS, Dimitrios A., Paschalis GKOUPIDENIS, Clemens STOLZ, Vivek SUBRAMANIAN, George G. MALLIARAS a David C. MARTIN. *Impedance Spectroscopy of Spin-Cast and Electrochemically Deposited PEDOT: PSS Films on Microfabricated Electrodes with Various Areas* [online]. [cit. 2018-09-26]. DOI: 10.1002/celc.201700297. ISBN 2196-0216.

[37] KANETO, Keiichi, Tanemasa ASANO, Wataru TAKASHIMA, et al. *Memory Device Using a Conducting Polymer and Solid Polymer Electrolyte: gelatin composites mediate brain endothelial cell adhesion* [online]. [cit. 2018-09-27]. DOI: 10.1143/JJAP.30.L215. ISBN 0021-4922.

[38] MATSUE, Tomokazu, Matsuhiko NISHIZAWA, Takahiro SAWAGUCHI, et al. *An enzyme switch sensitive to NADH: gelatin composites mediate brain endothelial cell adhesion* [online]. [cit. 2018-09-27]. DOI: 10.1039/C39910001029. ISBN 0022-4936.

[39] SAXENA, Vibha, Vinay SHIRODKAR, Rajiv PRAKASH, et al. *A comparative study of a polyindole-based microelectrochemical transistor in aqueous and non-aqueous electrolytes: gelatin composites mediate brain endothelial cell adhesion* [online]. [cit. 2018-09-27]. DOI: 10.1007/s100080050200. ISBN 1432-8488.

[40] TEHRANI, Payman, Nathaniel D ROBINSON, Thomas KUGLER, et al. Patterning polythiophene films using electrochemical over-oxidation: the origin, evolution, and impact of doi moi. *Advanced Materials* [online]. 2000 [cit. 2018-09-27]. DOI: 10.1088/0964-1726/14/4/N03. ISBN 0964-1726.

[41] PERINKA, Nikola, Chang Hyun KIM, Marie KAPLANOVA, et al. Preparation and Characterization of Thin Conductive Polymer Films on the base of PEDOT: PSS by Ink-Jet Printing. *Advanced Materials* [online]. 2000 [cit. 2018-09-27]. DOI: 10.1016/j.phpro.2013.04.016. ISBN 1875-3892.

[42] PERINKA, Nikola, Chang Hyun KIM, Marie KAPLANOVA, et al. Preparation and Characterization of Thin Conductive Polymer Films on the base of PEDOT: PSS by Ink-Jet Printing. *Advanced Materials* [online]. 2000 [cit. 2018-09-27]. DOI: 10.1002/app.42359. ISBN 1875-3892.

[43] GUALANDI, I., M. MARZOCCHI, A. ACHILLI, et al. Textile Organic Electrochemical Transistors as a Platform for Wearable Biosensors: PSS by Ink-Jet Printing. *Advanced Materials* [online]. 2000 [cit. 2018-09-27]. DOI: 10.1038/srep33637. ISBN 2045-2322.

[44] WILLIAMSON, Adam, Marc FERRO, Pierre LELEUX, et al. *Localized Neuron Stimulation with Organic Electrochemical Transistors on Delaminating Depth Probes* [online]. [cit. 2018-10-01]. DOI: 10.1002/adma.201500218. ISBN 0935-9648.

[45] LEE, Wonryung, Dongmin KIM, Jonathan RIVNAY, et al. *Integration of Organic Electrochemical and Field-Effect Transistors for Ultraflexible, High Temporal Resolution Electrophysiology Arrays* [online]. [cit. 2018-10-01]. DOI: 10.1002/adma.201602237. ISBN 0935-9648.

[46] CAMPANA, Alessandra, Tobias CRAMER, Daniel T. SIMON, Magnus BERGGREN a Fabio BISCARINI. *Electrocardiographic Recording with Conformable Organic Electrochemical Transistor Fabricated on Resorbable Bioscaffold* [online]. [cit. 2018-10-01]. DOI: 10.1002/adma.201400263. ISBN 0935-9648.

[47] LELEUX, Pierre, Jonathan RIVNAY, Thomas LONJARET, Jean-Michel BADIER, Christian BÉNAR, Thierry HERVÉ, Patrick CHAUVEL a George G. MALLIARAS. *Organic Electrochemical Transistors for Clinical Applications* [online]. [cit. 2018-10-01]. DOI: 10.1002/adhm.201400356. ISBN 2192-2640.

[48] YAO, Chunlei, Changyan XIE, Peng LIN, Feng YAN, Pingbo HUANG a I-Ming HSING. *Organic Electrochemical Transistor Array for Recording Transepithelial Ion Transport of Human Airway Epithelial Cells* [online]. [cit. 2018-10-01]. DOI: 10.1002/adma.201302615. ISBN 0935-9648

[49] GU, Xi, Chunlei YAO, Ying LIU a I-Ming HSING. *16-Channel Organic Electrochemical Transistor Array for In Vitro Conduction Mapping of Cardiac Action Potential* [online]. [cit. 2018-10-01]. DOI: 10.1002/adhm.201600189. ISBN 2192-2640.

[50] FARIA, Gregório C., Duc T. DUONG, Alberto SALLEO, Christos A. POLYZOIDIS, Stergios LOGOTHETIDIS, Jonathan RIVNAY, Roisin OWENS a George G. MALLIARAS. *Organic electrochemical transistors as impedance biosensors* [online]. [cit. 2018-10-01]. DOI: 10.1557/mrc.2014.35. ISBN 2159-6859.

[51] ZHANG, Yi, Sahika INAL, Chih-Yun HSIA, Magali FERRO, Marc FERRO, Susan DANIEL a Roisin M. OWENS. *Supported Lipid Bilayer Assembly on PEDOT: PSS Films and Transistors* [online]. [cit. 2018-10-01]. DOI: 10.1002/adfm.201602123. ISBN 1616-301X.

[52] RAMUZ, Marc, Adel HAMA, Miriam HUERTA, Jonathan RIVNAY, Pierre LELEUX a Róisín M. OWENS. *Combined Optical and Electronic Sensing of Epithelial Cells Using Planar Organic Transistors* [online]. [cit. 2018-10-01]. DOI: 10.1002/adma.201401706. ISBN 0935-9648.

[53] TRIA, Scherrine A., Marc RAMUZ, Miriam HUERTA, et al. *Dynamic Monitoring of Salmonella typhimurium Infection of Polarized Epithelia Using Organic Transistors* [online]. [cit. 2018-10-01]. DOI: 10.1002/adhm.201300632. ISBN 2192-2640.

[54] BOLIN, Maria H., Karl SVENNERSTEN, David NILSSON, Anurak SAWATDEE, Edwin W. H. JAGER, Agneta RICHTER-DAHLFORS a Magnus BERGGREN. *Active Control of Epithelial Cell-Density Gradients Grown Along the Channel of an Organic Electrochemical Transistor* [online]. [cit. 2018-10-01]. DOI: 10.1002/adma.200901191. ISBN 0935-9648.

[55] WAN, Alwin Ming-Doug, Sahika INAL, Tiffany WILLIAMS, et al. *3D conducting polymer platforms for electrical control of protein conformation and cellular functions* [online]. [cit. 2018-10-01]. DOI: 10.1039/C5TB00390C. ISBN 2050-750X.

[56] LIN, Peng, Xiaoteng LUO, I-Ming HSING a Feng YAN. *Organic Electrochemical Transistors Integrated in Flexible Microfluidic Systems and Used for Label-Free DNA Sensing* [online]. [cit. 2018-10-01]. DOI: 10.1002/adma.201102017. ISBN 0935-9648.

[57] ZAOUK, Rabih, Benjamin Y. PARK a Marc J. MADOU. *Introduction to Microfabrication Techniques* [online]. [cit. 2018-10-01]. DOI: 10.1385/1-59259-997-4:3. ISBN 15-925-9997-4.

[58] KAWASE, T., SIRRINGHAUS a T. SHIMODA. Inkjet Printed Via-Hole Interconnections and Resistors for All-Polymer Transistor Circuits. *Advanced Materials* [online]. 2001, 13(21) [cit. 2016-02-02]. DOI: 10.1002/1521-4095(200111)13:21<1601::AID-ADMA1601>3.0.CO;2-X.

[59] YOSHIOKA, Yuka, Paul D. CALVERT a Ghassan E. JABBOUR. *Simple Modification of Sheet Resistivity of Conducting Polymeric Anodes via Combinatorial Ink-Jet Printing Techniques* [online]. [cit. 2018-10-01]. DOI: 10.1002/marc.200400527. ISBN 1022-1336.

[60] LIU, Yi, Kody VARAHRAMYAN a Tianhong CUI. *Low-Voltage All-Polymer Field-Effect Transistor Fabricated Using an Inkjet Printing Technique* [online]. [cit. 2018-10-01]. DOI: 10.1002/marc.200500493. ISBN 1022-1336.

[61] BAO, Zhenan, Yi FENG, Ananth DODABALAPUR, V. R. RAJU a Andrew J. LOVINGER. *High-Performance Plastic Transistors Fabricated by Printing Techniques* [online]. [cit. 2018-10-01]. DOI: 10.1021/cm9701163. ISBN 0897-4756.

[62] GARNIER, F., R. HAJLAOUI, A. YASSAR a P. SRIVASTAVA. All-Polymer Field-Effect Transistor Realized by Printing Techniques. *Science* [online]. 1994, 265(5179), 1684-1686 [cit. 2018-10-01]. DOI: 10.1126/science.265.5179.1684. ISSN 0036-8075.

[63] PARDO, D. A., G. E. JABBOUR a PEYGHAMBARIAN. Application of Screen Printing in the Fabrication of Organic Light-Emitting Devices. *Advanced Materials* [online]. 2000, 12(17), 1249-1252 [cit. 2018-10-01]. DOI: 10.1002/1521-4095(200009)12:17<1249::AID-ADMA1249>3.0.CO;2-Y.

[64] EHLICH, Jiří. *Příprava organických elektrochemických tranzistorů pro biosenzoriku* [online]. Brno, 2015 [cit. 2018-10-02]. Dostupné z: https://www.vutbr.cz/studenti/zav-prace/detail/74159. Bakalářská práce. Fakulta Chemická, VUT v Brně. Vedoucí práce Doc. Ing. Ota Salyk, CSc.

[65] EHLICH, jiří. *Optimalizace tiskových metod přípravy organických polovodivých vrstev* [online]. Brno, 2017 [cit. 2018-10-02]. Dostupné z: https://www.vutbr.cz/studenti/zav-prace/detail/98442. Diplomová práce. Fakulta Chemická, VUT v Brně. Vedoucí práce Doc. Ing. Ota Salyk, CSc.

[66] ALEMU, Desalegn, Hung-Yu WEI, Kuo-Chuan HO a Chih-Wei CHU. *Highly conductive PEDOT: PSS electrode by simple film treatment with methanol for ITO-free polymer solar cells* [online]. [cit. 2018-10-02]. DOI: 10.1039/C2EE22595F. ISBN 1754-5692.

[67] ŠAFAŘÍKOVÁ, Eva. *Testování biokompatibility materiálů pro experimentální práci v buněčné biologii* [online]. Brno, 2016 [cit. 2018-10-02]. Dostupné z: https://is.muni.cz/th/sfmls/?so=nx. Diplomová práce. Přírodovědecká fakulta, Masarykova univerzita. Vedoucí práce Mgr. Jan Víteček, Ph.D.

[68] SALYK, Ota, Jan VÍTEČEK, Lukáš OMASTA, Eva ŠAFAŘÍKOVÁ, Stanislav STŘÍTESKÝ, Martin VALA a Martin WEITER. Organic Electrochemical Transistor Microplate for Real-Time Cell Culture Monitoring. Applied Sciences [online]. 2017, 7(10) [cit. 2018-11-05]. DOI: 10.3390/app7100998. ISSN 2076-3417.

[69] STŘÍTESKÝ, Stanislav, Aneta MARKOVÁ, Jan VÍTEČEK, et al. *Printing inks of electroactive polymer PEDOT: PSS* [online]. [cit. 2018-10-03]. DOI: 10.1002/jbm.a.36314. ISBN 1549-3296.

8 CURICULUM VITAE

Personal information

Name and Surname	Lukáš Omasta
Address:	Prvej SNR 250/7, 907 01 Myjava, Slovenská republika
Date of birth:	17. 01. 1989, Myjava
Phone number:	+420 604 294 274
E-mail:	xcomastal@fch.vutbr.cz

Education

2013 – present	Brno University of Technology, Faculty of Chemistry, Czech Republic Ph.D. study program Dissertation thesis: Printed biosensor based on organic electrochemical transistor
2011 – 2013	Brno University of Technology, Faculty of Chemistry, Czech Republic Master study program Master thesis: Příprava a charakterizace tenkých vrstev nízkomolekulárních materiálů pro organickou fotoniku
2008 – 2011	Brno University of Technology, Faculty of Chemistry, Czech Republic Bachelor study program Bachelor thesis: Organické solárne články na báze nízkomolekulárnych materiálov

Internship

08/2011 – 12/2011	Internship at the University of Trondheime, Norway (Norwegian University of Science and Technology), Erasmus program

Oral lectures at international conferences

7th meeting on Chemistry and Life 2018 (Brno, Czech Republic)
5th International Winterschool on Bioelectronics: BioEl 2018 (Kirchberg in Tirol, Austria)
17th Workshop of Physical Chemists and Electrochemist 2017 (Brno, Czech Republic)

Posters at international conferences

4th International Winterschool on Bioelectronics: BioEl 2017 (Kirchberg in Tirol, Austria)
12th International Conference on Organic Electronics (Bratislava, Slovak Republic)
6th meeting on Chemistry and Life 2015 (Brno, Czech Republic)
11th International Conference on Organic Electronics 2015 (Erlangen-Nurnberg, Germany)
7th International Symposium on Flexible Organic Electronics 2014 (Thessaloniki, Greece)
CEITEC Annual Conference “Frontiers in Material and Life Sciences” 2014 (Brno, Czech Republic)

Consultation of diploma theses

Jiří Ehlich	Optimalizace tiskových metod přípravy organických polovodivých vrstev

Consultation of bachelor theses

Jiří Ehlich	Příprava organických elektrochemických tranzistorů pro biosenzoriku

Aneta Brábliková	Optimalizace tisku organických elektronických struktur pro bioelektroniku

Pedagogical activity

2013 – present	Praktikum z fyziky – teacher in laboratory exercises
2016 – 2017	Complementary pedagogical studies

Articles in an impacted journals

SALYK, Ota, Jan VÍTEČEK, Lukáš OMASTA, Eva ŠAFAŘÍKOVÁ, Stanislav STŘÍTESKÝ, Martin VALA a Martin WEITER. Organic Electrochemical Transistor Microplate for Real-Time Cell Culture Monitoring. Applied Sciences [online]. 2017, 7(10) [cit. 2018-11-05]. DOI: 10.3390/app7100998. ISSN 2076-3417.

HRABAL, Michal, Ivaylo ZHIVKOV, Lukáš OMASTA, Klára FOLDÝNOVÁ, Patrícia GURICOVÁ, Martin VALA a Martin WEITER. Solid-state fluorescence organic materials as a tool for spectral modification of ZnS-based screen-printed thick layer electroluminescence devices. Chemical Papers [online]. 2018, 72(7), 1677-1684 [cit. 2018-11-21]. DOI: 10.1007/s11696-018-0404-z. ISSN 2585-7290.

Conference papers indexed in the Web of Science database

HRABAL, M.; ZHIVKOV, I.;TULIEV, N., DOBRIKOV, G., OMASTA, L.; VALA, M. Voltage source for AC electroluminescent measurements. In IEEE Xplore. Sozopol, Bulgaria: IEEE, 2017. s. 1-4. ISBN: 978-1-5386-1753-3.

SALYK, Ota, Lukáš OMASTA, Martin VALA a Martin WEITER. Organic Sensor for Cardiomyocytes Research. Materials Science Forum [online]. 2016, 851, 194-198 [cit. 2018-11-21]. DOI: 10.4028/www.scientific.net/MSF.851.194. ISSN 1662-9752.

Conference papers and abstracts

OMASTA, L.; SALYK, O.; VALA, M.; WEITER, M. Screen printing of organic electrochemical transistor for cardiomyocytes research. Studentská odborná konference Chemie je život 2015, Sborník abstraktů. Brno: Vysoké učení technické v Brně, Fakulta chemická, Purkyňova 464/118, 612 00 Brno, 2015. s. 375-380. ISBN: 978-80-214-5290- 9.

STŘÍTESKÝ, S.; OMASTA, L.; TUMOVÁ, Š.; ŠAFAŘÍKOVÁ, E.; VÍTEČEK, J.; SALYK, O.; VALA, M.; WEITER, M. High resolution gold printed electrodes for cell culture monitoring by OECT transistors. Kirchberg in Tirol, Austria: 2018. s. 85-85.

OMASTA, L.; EHLICH, J.; STŘÍTESKÝ, S.; SALYK, O.; VALA, M.; WEITER, M. Organic Electrochemical Transistor for Cell Culture Investigation. Kirchberg in Tirol, Austria: 2018. s. 51-51.

OMASTA, L.; SALYK, O.; STŘÍTESKÝ, S.; HRABAL, M.; VALA, M.; WEITER, M. Organic electrochemical transistors for real-time cell culture monitoring. Kirchberg in Tirol, Austria: 2017. s. 70-70.

OMASTA, L.; SALYK, O.; STŘÍTESKÝ, S.; HRABAL, M.; VALA, M.; WEITER, M. Organic electrochemical transistors for real-time cell observation. XVII. Workshop of Physical Chemists and Electrochemists Book of abstracts. 1. Brno: Masaryk University, 2017. s. 41-41. ISBN: 978-80-210-8580-0.

OMASTA, L.; SALYK, O.; STŘÍTESKÝ, S.; HRABAL, M.; VALA, M.; WEITER, M. Screen printing of organic electrochemical transistor for real-time cell culture monitoring. Sborník abstraktů. 1. Brno: Vysoké učení technické v Brně, Fakulta chemická, Purkyňova 464/118, 612 00 Brno, 2017. s. 88-88. ISBN: 978-80-214-5488-0.

OMASTA, L.; HRABAL, M.; SALYK, O.; VALA, M.; WEITER, M. Printed lateral biosensors based on organic electrochemical transistor. Book of Abstracts of The 12th International Conference on Organic Electronics. Bratislava, Slovakia: Slovak University of Technology in Bratislava, 2016. s. 57-57. ISBN: 978-80-227-4571- 0.

HRABAL, M.; OMASTA, L.; VALA, M.; SALYK, O.; WEITER, M. Printing of thin films for printed electronics. Book of Abstracts of The 12th International Conference on Organic Electronics. Bratislava, Slovakia: Slovak University of Technology in Bratislava, 2016. s. 31-31. ISBN: 978-80-227-4571- 0.

OMASTA, L.; SALYK, O.; HRABAL, M.; WEITER, M. Preparation and optimization of printed layers for biosensing. Chemistry & Life 2015 - Book of Abstracts. first. Brno: Brno University of Technology, Faculty of Chemistry, 2015. s. 140-140. ISBN: 978-80-214-5228- 2.

HRABAL, M.; OMASTA, L.; VALA, M.; WEITER, M. Optimization of Screen Printing Process for Printed Electronic Devices. Chermistry and Life Brno 2015. 2015. s. 138-139. ISBN: 978-80-214-5228- 2.

HRABAL, M.; OMASTA, L.; VALA, M. Preparation of organic electrochemical transistors via screen printing. Book of Abstracts 11th International Conference on Organic Electronics. První. Erlangen-Nurnberg, Germany: Friedrich- Alexander Universitat, 2015. s. 25-25.

SALYK, O.; OMASTA, L.; VALA, M.; WEITER, M. Printed Organic Sensor for Cardiomyocytes Research. Chemistry & Life 2015 , Book of Abstracts. first. Brno: Faculty of Chemistry, Brno University of Technology, 2015. s. 147-147. ISBN: 978-80-214-5228- 2.

OMASTA, L.; SALYK, O.; HRABAL, M.; WEITER, M. Printed biosensors based on organic electrochemical transistors. Book of Abstracts 11th International Conference on Organic Electronics. První. Erlangen-Nurnberg, Nemecko: Friedrich- Alexander Universitat, 2015. s. 58-58.

OMASTA, L.; SALYK, O.; WEITER, M. Electrochemical transistors based on inkjet printed PEDOT: PSS for biosensing. Book of Abstracts CEITEC Annual Conference “Frontiers in Material and Life Sciences”. První edice. Brno: Masarykova Univerzita, 2014. s. 189-189. ISBN: 978-80-210-7159- 9

OMASTA, L.; SALYK, O.; WEITER, M. Inkjet printed organic electrochemical transistors for biosensing. Studentská odborná konference Chemie je život 2014, Sborník abstraktů. Purkyňova 464/118, 612 00Brno: Vysoké učení technické v Brně, Fakulta chemická, 2014. s. 85-85. ISBN: 978-80-214-5077- 6.

OMASTA, L.; SALYK, O.; WEITER, M. Preparation of inkjet printed electrochemical transistors based on poly(3,4-ethylenedioxythiophene) polystyrene sulfonate. 2014. s. 156-156.

Brno 15. 3. 2019